Gastroenterology 2020;159:169–182

Innate Immune Molecule NLRC5 Protects Mice From *Helicobacter*-induced Formation of Gastric Lymphoid Tissue

Michelle Chonwerawong,[1,2] Jonathan Ferrand,[1] Hassan Mohammad Chaudhry,[1] Chloe Higgins,[1] Le Son Tran,[1] San Sui Lim,[1] Marjorie M. Walker,[3,4] Prithi S. Bhathal,[4] Anouk Dev,[5] Gregory T. Moore,[5] William Sievert,[5,6] Brendan J. Jenkins,[1,2] Mario M. D'Elios,[6] Dana J. Philpott,[7] Thomas A. Kufer,[8] and Richard L. Ferrero[1,2,9]

[1]Centre for Innate Immunity and Infectious Diseases, Hudson Institute of Medical Research, Victoria, Australia; [2]Department of Molecular and Translational Science, Monash University, Victoria, Australia; [3]School of Medicine and Public Health, Faculty of Health and Medicine, The University of Newcastle, New South Wales, Australia; [4]Department of Pathology, University of Melbourne, Victoria, Australia; [5]Department of Medicine, Monash University, Monash Medical Centre, Victoria, Australia; [6]Dipartimento di Medicina Sperimentale e Clinica, University of Florence, Florence, Italy; [7]Department of Immunology, University of Toronto, Toronto, Ontario, Canada; [8]University of Hohenheim, Institute of Nutritional Medicine, Department of Immunology, Stuttgart, Germany; and [9]Biomedicine Discovery Institute, Department of Microbiology, Monash University, Victoria, Australia

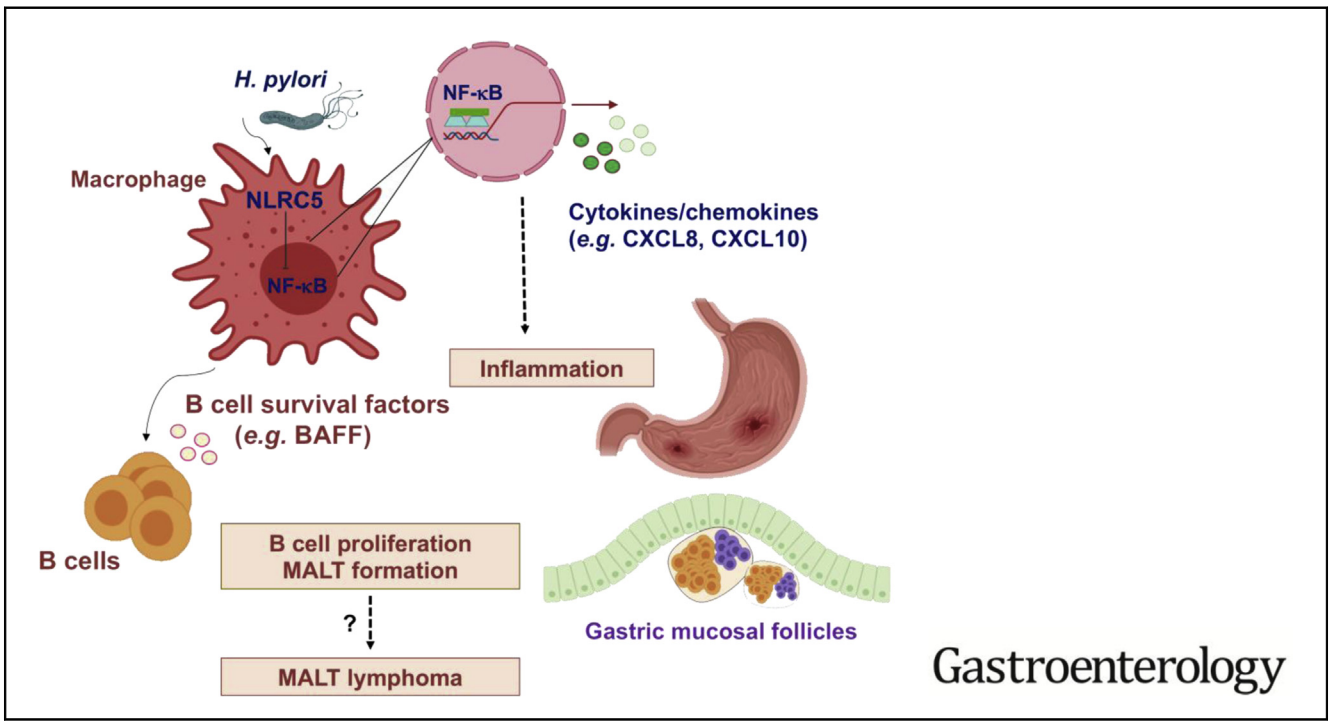

BACKGROUND & AIMS: *Helicobacter pylori* induces strong inflammatory responses that are directed at clearing the infection, but if not controlled, these responses can be harmful to the host. We investigated the immune-regulatory effects of the innate immune molecule, nucleotide-binding oligomerization domain-like receptors (NLR) family CARD domain-containing 5 (NLRC5), in patients and mice with *Helicobacter* infection. **METHODS:** We obtained gastric biopsies from 30 patients in Australia. We performed studies with mice that lack NLRC5 in the myeloid linage ($Nlrc5^{m\phi KO}$) and mice without *Nlrc5* gene disruption (controls). Some mice were gavaged with *H pylori* SS1 or *Helicobacter felis*; 3 months later, stomachs, spleens, and sera were collected, along with macrophages derived from bone marrow. Human and mouse gastric tissues and mouse macrophages were analyzed by histology, immunohistochemistry, immunoblots, and quantitative polymerase chain reaction. THP-1 cells (human macrophages, controls) and $NLRC5^{-/-}$ THP-1 cells (generated by CRISPR-Cas9 gene editing) were incubated with *Helicobacter* and gene expression and production of cytokines were analyzed. **RESULTS:** Levels of *NLRC5* messenger RNA were significantly increased in gastric tissues from patients with *H pylori* infection, compared with patients without infection ($P < .01$), and correlated with gastritis severity ($P < .05$). *H pylori* bacteria induced significantly higher levels of chemokine and cytokine production by $NLRC5^{-/-}$ THP-1 macrophages than by control THP-1 cells ($P < .05$). After 3 months of infection with *H felis*, $Nlrc5^{m\phi\text{-}KO}$ mice developed gastric hyperplasia ($P < .0001$), splenomegaly ($P < .0001$),

and increased serum antibody titers ($P < .01$), whereas control mice did not. *Nlrc5*$^{mø\text{-}KO}$ mice with chronic *H felis* infection had increased numbers of gastric B-cell follicles expressing CD19 ($P < .0001$); these follicles had features of mucosa-associated lymphoid tissue lymphoma. We identified B-cell–activating factor as a protein that promoted B-cell hyperproliferation in *Nlrc5*$^{mø\text{-}KO}$ mice. **CONCLUSIONS:** NLRC5 is a negative regulator of gastric inflammation and mucosal lymphoid formation in response to *Helicobacter* infection. Aberrant NLRC5 signaling in macrophages can promote B-cell lymphomagenesis during chronic *Helicobacter* infection.

Keywords: MALT lymphoma; BAFF; B-lymphocytes; Gastric Carcinogenesis.

WHAT YOU NEED TO KNOW

BACKGROUND AND CONTEXT

Helicobacter pylori induces strong inflammatory responses that are directed at clearing the infection, but if not controlled, these responses can be harmful

NEW FINDINGS

In studies of gastric tissues from patients and mice, we found that NLRC5 is a negative regulator of gastric inflammation and mucosal lymphoid formation in response to *Helicobacter* infection. Aberrant NLRC5 signaling in macrophages can promote B-cell lymphomagenesis during chronic *Helicobacter* infection.

LIMITATIONS

This study was performed using human tissues and mice.

IMPACT

NLRC5 in macrophage is an important regulator of the gastric inflammatory response to *Helicobacter* infection

The gut microbiota influences innate and adaptive responses that are important for the maintenance of mucosal immunohomeostasis, which, if disrupted, may lead to gastrointestinal disease.[1] Immune responses can protect the host against infection, but may also have a major influence on disease outcome.[2,3] One example is the bacterium *Helicobacter pylori,* which despite colonizing the stomach for decades, is generally not associated with symptomatology or serious sequelae, yet is a major causal factor in peptic ulcer disease and gastric cancer. It is now accepted that the chronic gastritis induced by *H pylori* infection plays a central role in the development of adenocarcinoma.[4] Prolonged inflammation in *H pylori*–infected subjects also promotes the formation of lymphoepithelial lesions and mucosal lymphoid follicles, typically composed of B-lymphocytes.[5,6] These follicles may develop into gastric B-cell mucosa-associated lymphoid tissue (MALT) lymphoma.[5,6] Approximately 92% to 98% of cases of gastric MALT lymphoma are associated with *H pylori*–induced gastritis.[6] Lesions resembling human gastric B-cell MALT lymphoma have been shown to develop in mice with chronic *Helicobacter* infection, in particular those associated with *Helicobacter felis.*[7,8]

Macrophages play a crucial role in regulating inflammatory responses during chronic *H pylori* infection.[9–11] Monocytes and macrophages secrete cytokines that drive the polarization of T helper (Th) responses to a Th1 phenotype and the production of interferon-γ (IFN-γ) by CD4$^+$ T cells.[12] Macrophages also shape adaptive immune responses to *Helicobacter* infection, by acting as antigen-presenting cells and secreting B-cell survival factors, such as B-cell–activating factor (BAFF) and a proliferative-inducing ligand (APRIL).[13,14] BAFF and APRIL secretion by mucosal macrophages mediates lymphocyte proliferation and B-cell lymphomagenesis during chronic *H pylori* infection.[13,14] Although some aspects of *Helicobacter*-induced gastric B-cell MALT lymphoma have been studied in detail,[14–16] current understanding of its pathogenesis is incomplete.

Nucleotide-binding oligomerization domain (NOD)-like receptors (NLRs) are a family of cytosolic pattern recognition receptors that regulate host defense responses against microorganisms.[17] Defects in NLR-mediated signaling, however, can disrupt immunohomeostasis, resulting in detrimental effects on the host.[17] One of these proteins, NLR family CARD domain-containing 5 (NLRC5), was proposed to function as a regulator of proinflammatory responses to intracellular bacterial and viral pathogens.[18–20] NLRC5 is strongly expressed in the myeloid cell lineage[18,19,21] and transactivates major histocompatibility complex (MHC) class I genes to mediate antitumor activity.[22] It has been suggested that NLRC5 may be a positive prognostic marker for various cancers.[22]

IFN-γ plays a critical role in the Th-1-dependent inflammation associated with *H pylori* disease.[23] Given that IFN-γ also upregulates *NLRC5* expression,[18] thereby potentially promoting its antitumor activity,[22] we sought to determine the role of NLRC5 in gastric inflammation due to chronic *H pylori* infection. We now show that *H pylori* upregulates *NLRC5* expression in macrophages and gastric tissues. Furthermore, macrophage-specific NLRC5 was found to negatively regulate proinflammatory cytokine responses and to protect against the formation of mucosal B-cell lymphoid tissue formation in response to chronic *Helicobacter* infection in mice. We identified macrophage-derived BAFF as a key factor promoting B-cell lymphoid tissue formation in mice lacking functional Nlrc5 in the myeloid cell compartment. Thus, this work reveals a new role for NLRC5 as a potential suppressor of B-cell

Abbreviations used in this paper: **APRIL, a proliferative-inducing ligand; BAFF, B-cell–activating factor; BMDM, bone marrow–derived macrophage; ELISA, enzyme-linked immunosorbent assay; IFN-γ, interferon-γ; Ig, immunoglobulin; IL-1β, interleukin-1β; LPS, lipopolysaccharide; MHC, major histocompatibility complex class; MALT, mucosa-associated lymphoid tissue; MOI, multiplicity of infection; NLRC5, NLR family CARD domain-containing 5; NF-κB, nuclear factor-κB; NLR, nucleotide-binding oligomerization domain (NOD)-like receptor; p.i., postinfection; qRT-PCR, quantitative reverse-transcription polymerase chain reaction; STAT, signal transducer and activator of transcription; Th, T helper; WT, wild type.**

Most current article

0016-5085/$36.00
https://doi.org/10.1053/j.gastro.2020.03.009

lymphomagenesis and suggests that aberrant NLRC5 signaling may promote the development of MALT lymphoma associated with chronic *H pylori* infection.

Materials and Methods

Human Gastric Biopsies

Gastric biopsies were collected from consenting participants (n = 30) attending the Monash Medical Centre Gastrointestinal and Liver Unit (Monash Health Human Research Ethics Committee project number 07174A). Biopsies were graded histologically, according to a revised version of the Sydney System.[24] Samples were stored at −80°C until analyzed. *H pylori* infection status was confirmed using specific 16S ribosomal RNA primers, as described previously.[24]

Mice

Mice were maintained at the Monash Animal Research Platform, Monash Medical Centre, under specific pathogen-free conditions. All animal procedures complied with the guidelines approved by Monash Medical Centre Animal Ethics Committee (MMCA/2015/43). Mice lacking *Nlrc5* in the myeloid linage ($Nlrc5^{m\phi\text{-}KO}$; n = 68) were generated on the C57BL/6 background by crossing $Nlrc5^{fl/fl}$ mice with LysM-Cre animals, resulting in a deletion of exon 4 which codes for the NOD (Supplementary Figure 1*A*). As wild-type (WT) controls (n = 50), we used $Nlrc5^{wt/wt}$ *x* LysM-cre or $Nlrc5^{fl/fl}$ C57BL/6 mice. The ratio of male:female mice was 58:60.

Isolation of Murine Bone Marrow–Derived Macrophages (BMDMs)

The femurs and tibias of mice were flushed using 23-gauge needles (BD Biosciences, San Jose, CA). Cells were washed by centrifugation at 200*g* for 5 minutes, then resuspended in Dulbecco's modified Eagle's medium containing 10% (vol/vol) fetal calf serum, 1% (vol/vol) penicillin/streptomycin, 1% (vol/vol) L-glutamine (ThermoFisher Scientific, Scoresby, VIC, Australia) and 10% (vol/vol) L929-cell-conditioned medium. BMDMs were cultured in low adherence flasks (Sarstedt, Numbrecht, Germany) and incubated at 37°C in 5% CO_2 for 6 days.

Cell Lines

NLRC5-deficient ($NLRC5^{-/-}$) THP-1 cells were generated by CRISPR-Cas9 gene editing. $NLRC5^{-/-}$ and WT THP-1 cells, as well as human gastric epithelial AGS and MKN28 cell lines,[25] were maintained in RPMI medium supplemented with 10% (vol/vol) fetal calf serum, 1% (vol/vol) penicillin/streptomycin, and 1% (vol/vol) L-glutamine.

Bacterial Culture

H pylori Sydney Strain 1 (SS1),[26] *H felis* (ATCC 49179/CS1),[27] and *H pylori* clinical isolates associated with MALT lymphoma (189, 213, 223, 245), nonulcer dyspepsia (240, 244, 249, 251), or duodenal ulcer (DU, 246, 247, 250, 256)[25] were grown using standard methods.[28]

Cell Co-Culture Assays

BMDMs were seeded in 12-well plates (2×10^5 cells/mL) and incubated at 37°C, 5% CO_2 for 6 hours. Cells were serum-starved overnight before performing co-culture assays. Phorbol 12-myristate 13-acetate–treated (20 ng/mL; Sigma Aldrich, Saint Louis, MO) WT and $NLRC5^{-/-}$ THP-1 cells were seeded in 12-well plates (5×10^5 cells/mL) and incubated at 37°C, 5% CO_2 for 48 hours. Cells were serum-starved at least 1 hour before treatment. Liquid cultures of *H pylori* and *H felis* were used for co-culture assays at a multiplicity of infection [MOI] = 10:1, confirmed by viable counting.[28] Bacteria were heat-killed by treatment at 98°C for 1 hour. Bacteria were removed after 1 hour and the cells reincubated in fresh media. As controls, cells were treated with recombinant IFN-γ (100 ng/mL; BioLegend, San Diego, CA) or *Escherichia coli* O111: B4 lipopolysaccharide (LPS, 100 ng/mL; UltraPure, InvivoGen, San Diego, CA).

Quantitative Real-time Polymerase Chain Reaction (qRT-PCR)

Complementary DNA was synthesized from TURBO-DNase-treated (Thermo Fisher) RNA (500 ng) using the Tetro complementary DNA synthesis kit (Bioline, Eveleigh, NSW, Australia). qPCR reactions were performed on an Applied Biosystems (Foster City, CA) 7900 Fast Real-Time PCR machine (MHTP Medical Genomics Facility) using primers or Taqman probes (Supplementary Tables 1 and 2). Gene expression was compared by obtaining delta threshold cycle values (ΔCt) and normalizing to the expression of *RNA18S1/Rn18s*. Relative gene expression values were calculated as $2^{-\Delta\Delta Ct}$.

Cytokine Quantification

Enzyme-linked immunosorbent assay (ELISA) kits were used to quantify CXCL8 (interleukin [IL]-8) (BD Biosciences, NSW, Australia); IL-1β (ThermoFisher); tumor necrosis factor (BD Biosciences); keratinocyte chemoattractant/chemokine (C-X-C motif) ligand 1 (Cxcl1); macrophage inflammatory protein 2/Cxcl2; IFN-γ–induced protein 10/CXCL10); IFN-γ, APRIL, and BAFF (all R&D Systems, Minneapolis, MN). Absorbance values were measured at 450 nm with a FLUOStar Optima microplate reader (BMG Labtech, Mornington, VIC, Australia). Cytokine levels were determined by 4-parameter fit analysis.

In Vivo Infection

Mice (male and female; 6–8 weeks old) were orally gavaged with $>10^6$ colony-forming units of either *H pylori* SS1 or *H felis*.[28] As a control, mice were administered Brain Heart Infusion broth (ThermoFisher Scientific). Bacterial numbers were confirmed by agar plate dilution.[28] Mice were euthanized at 3 months postinfection (p.i.), and the stomachs, spleens, and sera collected.[28] *H pylori* SS1 colonization was expressed as colony-forming units per gram.[28] Formalin-fixed gastric tissue sections were stained with Harris' Hematoxylin and Eosin (H&E) (Amber Scientific, Midvale, Australia) or Wright Giemsa (Sigma-Aldrich, St Louis, MO) stains to assess histopathological changes or *H felis* colonization, respectively.[28] H&E-stained slides were analyzed using an Aperio slide scanner (×20 magnification) and ImageScope software (Leica Biosystems, Mount Waverley, VIC, Australia). Giemsa-stained slides were analyzed using an Olympus DP73 digital camera (×40 magnification) and CellSens

Dimension software (v1.7.1, Olympus Australia, Notting Hill, VIC, Australia). At least 2 tissue sections per slide were analyzed per mouse stomach.

Helicobacter-*specific Serum Antibody ELISA*

Antigen-specific antibody responses were determined using sonicated bacterial extracts (25 μg protein/well).[8] Anti-mouse secondary antibodies (diluted 1:5000; BD Biosciences) were added to plates for 2 hours at 37°C and immunoglobulins detected using streptavidin-peroxidase conjugate (BD Biosciences). *Helicobacter*-specific antibody endpoint titers for each treatment were determined relative to those of naïve mice.[8]

Statistical Analysis

GraphPad Prism 8 (GraphPad Software, La Jolla, CA) was used for all statistical analyses. Data were analyzed using the Mann-Whitney, Kruskal-Wallis, 1-way or 2-way analysis of variance tests, as indicated. Results are presented as mean ± standard error of the mean. P values <0.05 were considered statistically significant.

Results

Nlrc5/NLRC5 *Expression in Murine and Human Gastric Biopsies is Upregulated in Response to* H pylori *Infection*

Here, we reveal that *Nlrc5/NLRC5* expression is significantly increased in response to chronic *H pylori* infection in mouse and human gastric biopsies (Figure 1*A* and *B*, respectively). Furthermore, gastric *NLRC5* expression correlated positively with gastritis severity but not tumor formation, when compared with histologically normal and matched nontumor tissues, respectively (Figure 1*C*). As *NLRC5* expression is highly induced by IFN-γ,[18,29] a critical mediator of *H pylori*-gastritis,[23,24] we examined *IFNG* expression in these gastric biopsies. *IFNG* expression was highly induced in response to *H pylori* infection (Supplementary Figure 2*A*) and increased with disease severity (Supplementary Figure 2*B*). A correlation was also observed between *IFNG* and *NLRC5* expression, but this did not reach statistical significance (Supplementary Figure 2*C*). Thus, *Helicobacter* infection results in upregulated *NLRC5* expression in the gastric mucosa and this expression correlates with disease severity.

Helicobacters Upregulate Nlrc5/NLRC5 Expression in Murine and Human Macrophages

NLRC5 is responsive to a variety of microbe-associated molecular patterns, including LPS, resulting in the activation of type I IFN and Janus kinase/signal transducer and activator of transcription (STAT) signaling pathways.[19,29] We found that live *Helicobacter* bacteria induced the upregulation of *Nlrc5* expression in mouse BMDMs by 10- to 100-fold, comparable to the levels induced by IFN-γ and LPS (Figure 2*A*). *NLRC5* expression in THP-1–derived human macrophages was also significantly increased in response to *H pylori* and *H felis* stimulation, with maximal effects observed at 48 hours poststimulation (Figure 2*B* and data not shown). Interestingly, human gastric epithelial cell lines expressed *NLRC5* both basally and in response to stimulation, thus suggesting that NLRC5 in nonmyeloid cells may potentially be responsive to bacterial agonists (Supplementary Figure 3).

NLRC5 was located diffusely within the cytoplasm of untreated and IFN-γ–stimulated THP-1–derived macrophages (Figure 2*C*). In response to stimulation with either *H pylori* or *H felis*, NLRC5 formed well-defined aggregates (Figure 2*C*, low-power images) that localized to the perinuclear region of cells (Figure 2*C*, zoomed images). Collectively, these results show that *Helicobacter* bacteria upregulates *NLRC5/Nlrc5* expression in macrophages, resulting in the formation of perinuclear aggregates and the potential regulation of downstream signaling events.

NLRC5 is a Negative Regulator of Proinflammatory Reponses During Helicobacter *Infection*

NLRC5 has been reported to function as both a negative and positive regulator of inflammatory responses through its

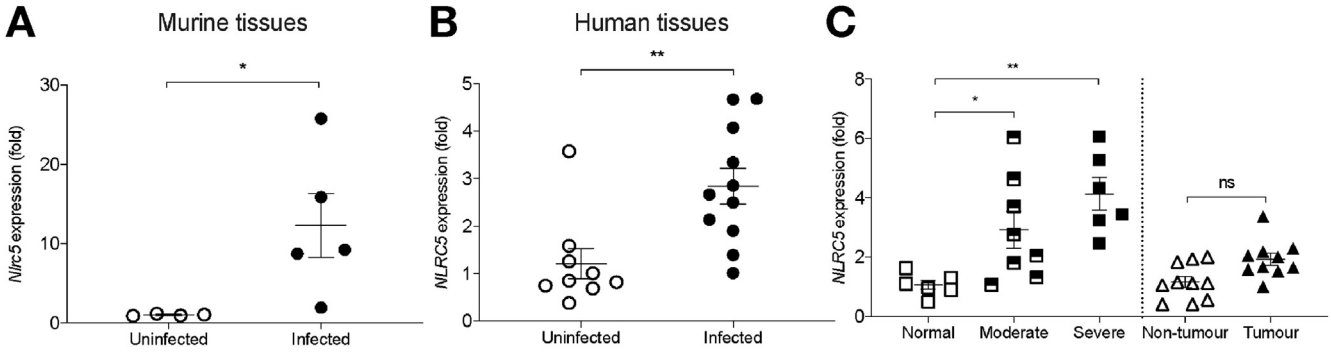

Figure 1. *Nlrc5/NLRC5* expression is upregulated in *H pylori*–infected murine and human gastric biopsies. (*A*) *Nlrc5* expression in murine gastric biopsies at 30 days p.i. with *H pylori* (n = 4–5 per group). (*B*) *NLRC5* expression in uninfected (control) and *H pylori*–infected human gastric biopsies. (*C*) *NLRC5* expression in human gastric biopsies classified as "normal," "moderate," or "severe" gastritis, and in nontumor/tumor tissues (n = 6–11 per group). *NLRC5* expression was normalized to uninfected or normal groups, respectively. Data are presented as the mean ± SEM. Values for individual murine or human gastric tissues are presented. Mann-Whitney (*A*, *B*) or Kruskal-Wallis (*C*) tests: $^*P < .05$, $^{**}P < .01$, and ns = not significant.

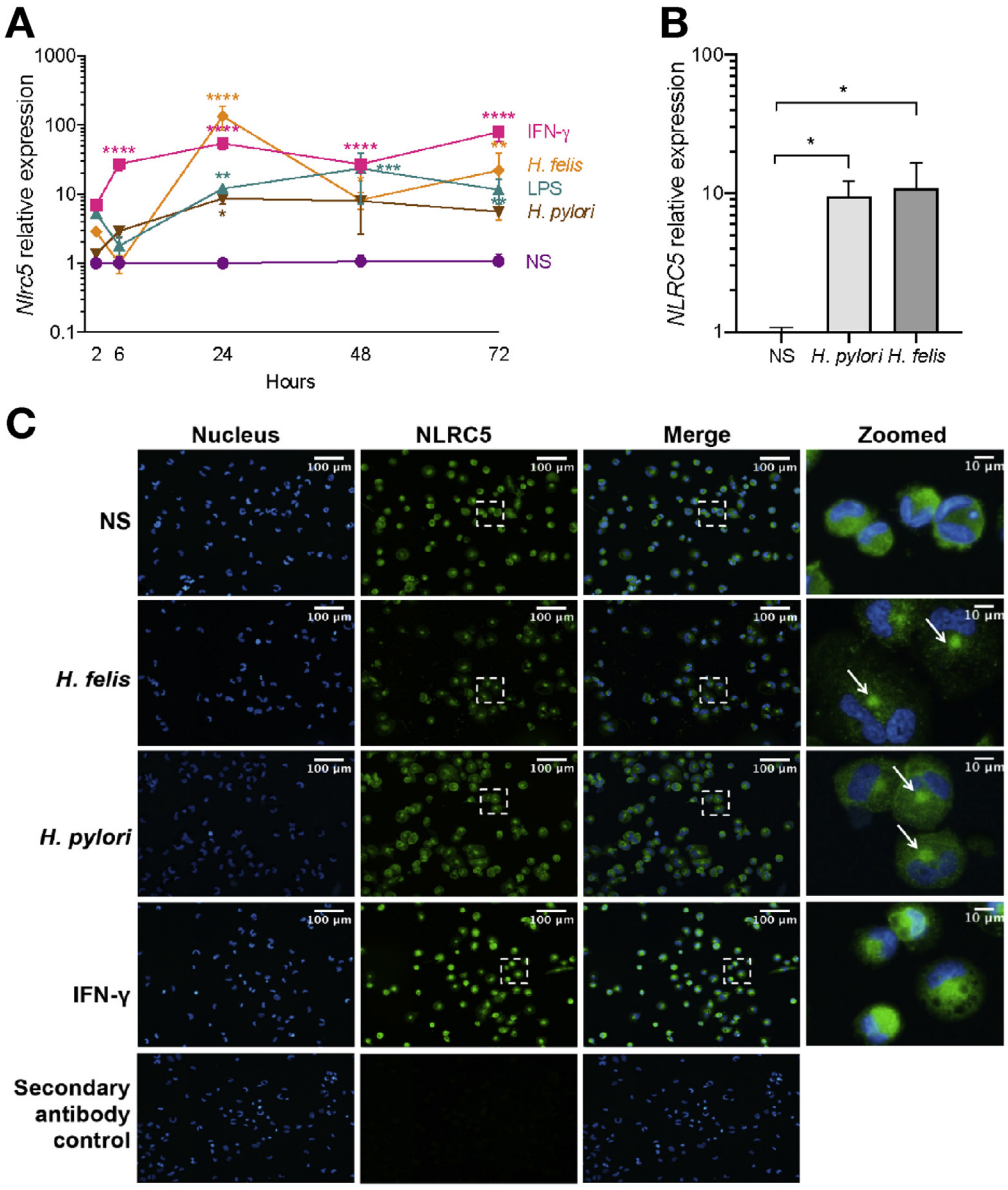

Figure 2. *Nlrc5/NLRC5* expression in macrophages is upregulated in response to live *Helicobacter* bacteria. (*A*) *Nlrc5* expression in murine BMDMs and (*B*) phorbol 12-myristate 13-acetate (PMA)-differentiated human monocytic THP-1 cells. Cells were either not stimulated (NS) or stimulated with recombinant IFN-γ (100 ng/mL), LPS (100 ng/mL), *H pylori* SS1, or *H felis* (MOI = 10). BMDMs and THP-1 cells were harvested at 2 to 72 and 48 hours, respectively. Data pooled from 3 and 7 independent experiments, respectively. Gene expression levels were normalized to *Rn18s* or *RNA18S1*, as appropriate. Data are presented as the mean ± SEM. Two-way analysis of variance or Kruskal-Wallis test, as appropriate: $^{**}P < .05$, $^{**}P < .01$, $^{***}P < .001$, $^{****}P < .0001$. (*C*) Detection of NLRC5 (*green*) and nuclei (*blue*) in NS and stimulated cells by immunofluorescence (scale bars, 100 and 10 μm). Secondary antibody alone–stained cells are shown as controls. *Arrows* indicate perinuclear aggregates of NLRC5. Representative images from 3 independent experiments.

effects on Janus kinase/STAT, Toll-like receptor, and IFN pathways.[18,29,30] Kumar et al[20] reported that NLRC5 was dispensable for cytokine induction in response to *Salmonella, Francisella,* and *Listeria* infection, whereas other authors found that NLRC5 was critical for the induction of $CD8^+$ T-cell responses against *Listeria* infection.[31] Thus, the role of NLRC5 in antimicrobial immune responses seems to depend on the particular infection model. To elucidate the role of NLRC5 in anti-*Helicobacter* responses, we used monocyte-derived WT and $NLRC5^{-/-}$ THP-1 macrophages (Figure 3*A*). Consistent with the role of NLRC5 as a transactivator of MHC class I genes,[32] we observed *HLAB* gene expression to be reduced in $NLRC5^{-/-}$ cells in response to stimulation with IFN-γ, LPS, *H pylori*, or *H felis* (Figure 3*B*). Conversely, these cells expressed increased levels of the MHC class II gene, *HLA-DRB*, both constitutively and in response to stimulation (Figure 3*C*).

The expression levels of nuclear factor-κB (NF-κB) target genes, *CXCL2* and *CXCL8*, were elevated in $NLRC5^{-/-}$ THP-1 macrophages stimulated with *Helicobacter* bacteria or known NLRC5 agonists (LPS, IFN-γ), when compared with WT cells (Figure 3*D* and *E*). Importantly, $NLRC5^{-/-}$ macrophages produced significantly more CXCL8, CXCL10, and IL-1β in response to stimulation with live *H pylori* or *H felis* bacteria (Figure 3*F–H*). These effects on chemokine production in $NLRC5^{-/-}$ THP-1 macrophages were also observed in response to stimulation with heat-killed bacteria (Supplementary Figure 4). Similar to the human macrophage data, the expression levels of several NF-κB–dependent cytokine and chemokine genes were upregulated in $Nlrc5^{m\text{ø-KO}}$ BMDMs in response to *H pylori* stimulation (Supplementary Figure 5*A–F*). *H pylori* clinical isolates associated with various disease outcomes, including MALT lymphoma, were equally able to upregulate proinflammatory responses in $NLRC5^{-/-}$ THP-1 cells (Supplementary Figure 5*I*).

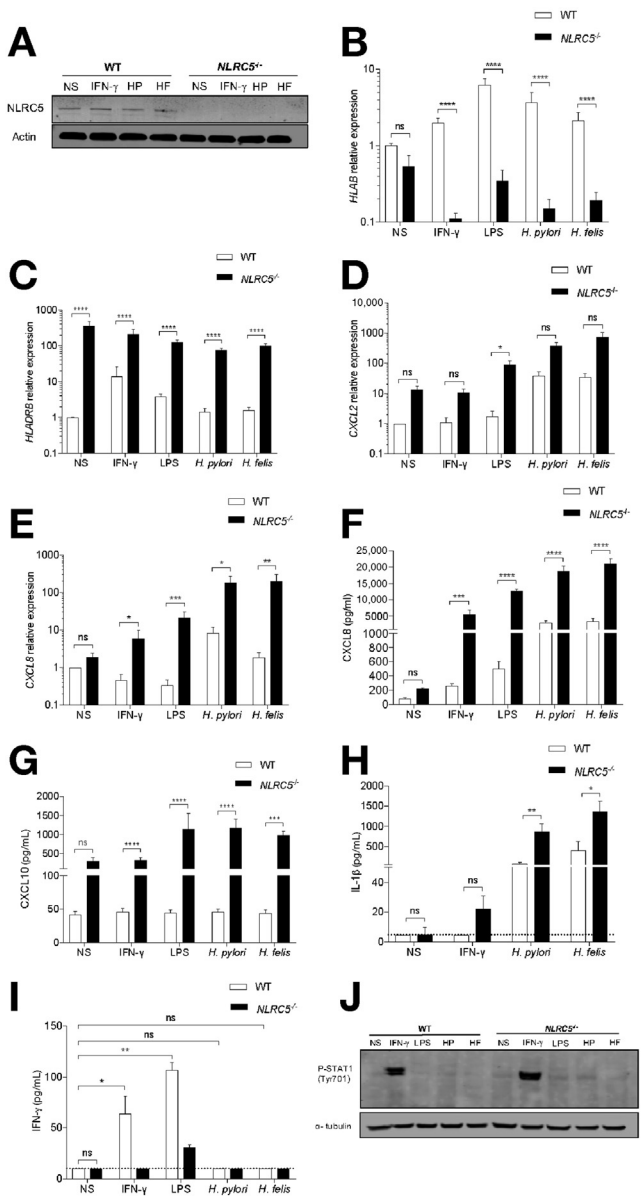

Figure 3. Increased immune responses of *NLRC5*$^{-/-}$ THP-1 cells to *Helicobacter* stimulation. (*A*) NLRC5 (204 kDa) was detected in WT and *NLRC5*$^{-/-}$ THP-1 cells that were either not stimulated (NS) or stimulated with *H felis* (HF) or *H pylori* SS1 (HP) (MOI = 10). β-Actin was used as a loading control. The image is representative of at least 3 independent experiments (n = 3). Gene expression levels in WT and *NLRC5*$^{-/-}$ THP-1 cells that were either not stimulated (NS) or stimulated with human recombinant IFN-γ (100 ng/mL), LPS (100 ng/mL), *H pylori* SS1, or *H felis* (MOI = 10). Detection of (*B*) *HLAB*, (*C*) *HLADRB*, (*D*) *CXCL2*, (*E*) *CXCL8*, (*F*) CXCL8, (*G*) IL-1β, (*H*) CXCL10, (*I*) IFN-γ, and (*J*) phosphorylated STAT1 (P-STAT1 Tyr701). Gene expression was normalized to that of *RNA18S1*. Tubulin was used as a loading control. Data are presented as the mean ± SEM from at least 3 independent experiments (n = 3). Kruskal-Wallis, 1-way or 2-way analysis of variance, as appropriate: **P* < .05, ***P* < .01, ****P* < .001, *****P* < .0001, and ns = not significant. Dotted lines represent values below the assay detection limit.

As IFN-γ is a known inducer of *NLRC5* expression,[18,29] we measured IFN-γ production in WT and *NLRC5*$^{-/-}$ THP-1 cells to determine whether the autocrine production of this cytokine may be responsible for upregulation of *NLRC5* expression in response to *Helicobacter* stimulation (Figure 2*B*). IFN-γ was produced in WT THP-1 cells that had been stimulated with either LPS or IFN-γ, but not those stimulated with *Helicobacter* bacteria (Figure 3*I*), thus indicating that autocrine IFN-γ is not involved in the inflammatory responses induced by these bacteria. Consistent with these data, phosphorylated (Tyr701)-STAT1 was not detected in cells stimulated with *Helicobacter* bacteria (Figure 3*J*). Taken together, the data suggest that NLRC5 acts to negatively regulate proinflammatory chemokine/cytokine responses to *Helicobacter* bacteria via a different mechanism to classical NLRC5 signaling.

NLRC5 Regulates Macrophage-secreted BAFF in Response to Helicobacter

The B-cell factors, BAFF and APRIL, are secreted by macrophages in response to *Helicobacter* infection and have been reported to be drivers of gastric B-cell MALT lymphoma.[13,14,33] Significantly higher *BAFF* expression levels were observed for *NLRC5*$^{-/-}$ THP-1 cells stimulated with LPS, *H pylori* or *H felis*, when compared with WT cells (Figure 4*A* and *B*). *BAFF* expression in response to either bacterial species was upregulated 10- to 100-fold (Figure 4*A*; Supplementary Figure 6) and maximal at 48 hours (Figure 4*A*). Although both species induced increased BAFF production in *NLRC5*$^{-/-}$ THP-1 cells, only those stimulated with *H felis* produced significantly more of this factor than WT cells (Figure 4*B*). *APRIL* gene expression was only increased in LPS-stimulated *NLRC5*$^{-/-}$ THP-1 cells when compared with WT cells (Figure 4*C* and *D*). No differences in APRIL protein levels were observed between the 2 cell lines. These findings suggest that macrophage-derived BAFF may be an important factor in NLRC5-mediated responses to *Helicobacter* infection.

NLRC5 Regulates Helicobacter*-induced Gastric Inflammation and Development of Mucosal Lymphoid Follicles*

NLRC5 is strongly expressed in myeloid cells[21] and downregulated proinflammatory responses to *Helicobacter* bacteria in vitro (Figure 3, Supplementary Figure 5*A*–*H*), we speculated that macrophage-derived NLRC5 may regulate inflammatory responses to *Helicobacter* infection in vivo. This question was addressed using conditional knockout mice with nonfunctional *Nlrc5* within the myeloid cell lineage (*Nlrc5*$^{\text{mø-KO}}$ mice). At 3 months p.i., mice were killed and their body weights and stomach mass were shown to be similar between WT and *Nlrc5*$^{\text{mø-KO}}$ animals (Supplementary Figure 7). Similarly, *Nlrc5* deficiency did not influence the bacterial burden within the stomachs of *H pylori*–infected *Nlrc5*$^{\text{mø-KO}}$ mice (Figure 5*A*). *H felis* infection status was verified by Giemsa staining fields (Figure 5*B*), as

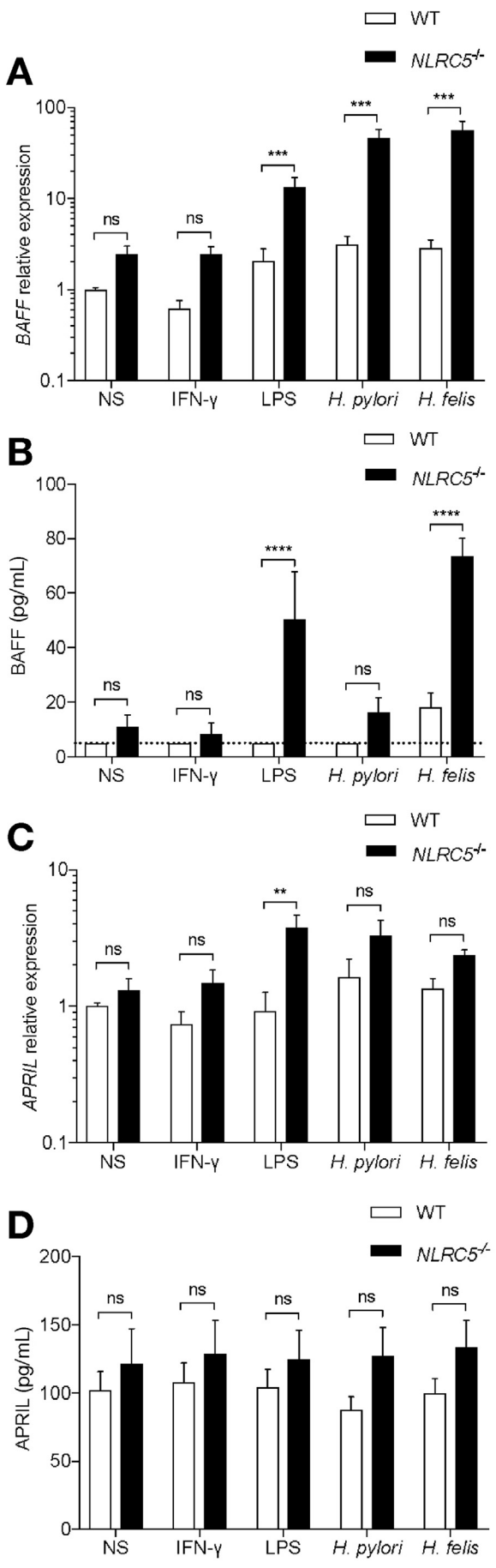

H felis does not form colonies on culture plates.[34] Although no significant differences in inflammatory responses were observed between WT and *Nlrc5*$^{mø\text{-}KO}$ mice with *H pylori* infection, *H felis*–infected *Nlrc5*$^{mø\text{-}KO}$ mice developed more severe inflammation and glandular hyperplasia when compared with WT animals (Figure 5*C–F*). A particularly noteworthy finding was that *H felis*–infected *Nlrc5*$^{mø\text{-}KO}$ mice also developed significantly higher numbers of lymphoid structures or follicles within the gastric mucosa (Figure 5*C–E*), consisting of predominantly B220^{+} cell populations and few CD3^{+} T cells (Figure 5*G*). This finding is consistent with the phenotype of follicles that form during gastric MALT lymphoma.[15]

Nlrc5$^{mø\text{-}KO}$ mice with chronic *Helicobacter* infection also demonstrated increased splenic mass compared with WT mice (Figure 5*H*). The spleen is one of the lymphoid organs that abundantly expresses *Nlrc5*[19,21] and is a major site for lymphoid cell proliferation. The serum of *Nlrc5*$^{mø\text{-}KO}$ mice also contained significantly elevated levels of *Helicobacter*-specific immunoglobulin (Ig)G, IgA, IgG1, and IgG2c antibodies when compared with WT animals (Figure 5*I–L*). Collectively, these results indicate that Nlrc5 functions to regulate the gastric inflammation associated with gastric B-cell lymphomagenesis in response to chronic *Helicobacter* infection, but does not appear to have a role in bacterial clearance. We suggest that NLRC5 may play a role in B-cell development in the spleen and other secondary lymphoid organs.

NLRC5 Controls B-Lymphocyte Proliferation in Murine Splenocytes During Chronic Helicobacter *Infection*

During gastric MALT lymphoma development, B cells within the marginal zones are thought to expand clonally, thus forming neoplastic lesions or lymphoid follicles in the gastric mucosa.[15] To investigate whether NLRC5 may regulate the B-cell proliferation required for gastric MALT lymphoma development, splenocytes from *H felis*–infected WT and *Nlrc5*$^{mø\text{-}KO}$ mice at 3 months p.i. were cultured ex vivo for 72 hours and labeled with the cell fluorescent dye, carboxyfluorescein succinimidyl ester, to monitor for lymphocyte proliferation. To observe whether factors secreted by murine macrophages in response to *H felis* stimulation may influence cell proliferation, conditioned media from nonstimulated or

Figure 4. Increased BAFF responses in *NLRC5*$^{-/-}$ THP-1 cells to *Helicobacter* stimulation. Monocyte-derived WT and *NLRC5*$^{-/-}$ THP-1 macrophages were either not stimulated (NS) or stimulated with human recombinant IFN-γ (100 ng/mL), LPS (100 ng/mL), *H pylori* SS1, or *H felis* (MOI = 10). Detection of (*A*) *BAFF* expression; (*B*) BAFF protein; (*C*) *APRIL* expression; and (*D*) APRIL protein. Gene expression was measured at 48 hours poststimulation and normalized to that of *RNA18S1*. BAFF and APRIL protein levels were determined at 48 and 72 hours, respectively. Data are presented as the mean ± SEM from at least 3 independent experiments (n = 3). Two-way analysis of variance test: $^{**}P < .01$, $^{***}P < .001$, $^{****}P < .0001$, and ns = not significant. *Dotted lines* represent values below the assay detection limit.

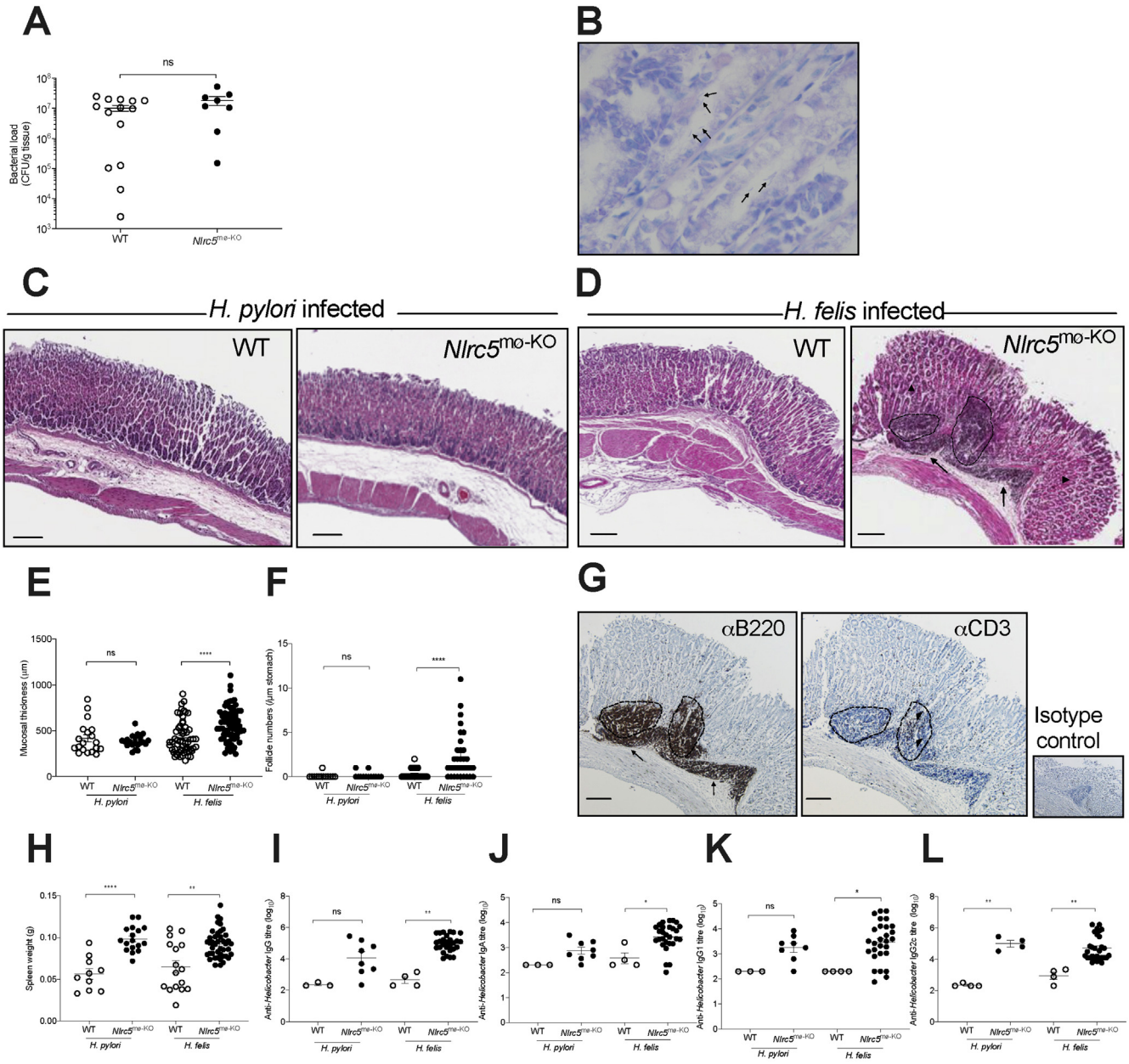

Figure 5. *Nlrc5*$^{mø\text{-}KO}$ mice exhibit increased inflammatory responses and accelerated gastric B-cell lymphoid formation in response to chronic *H felis* infection. (*A*) Bacterial burden of *H pylori* SS1 in the stomachs of mice at 3 months p.i. Colonies are quantified as colony-forming units per gram (CFU/g) of stomach tissue. Bacterial counts were plated in duplicate per mouse stomach, and the average CFU calculated (n = 8–14 mice per group). (*B*) *H felis*–infected murine gastric tissue with *arrows* showing the presence of the bacterium within gastric glands (Giemsa stain, magnification ×40). Histopathological changes in the stomachs of WT and *Nlrc5*$^{mø\text{-}KO}$ mice at 3 months p.i. with (*C*) *H pylori* SS1 or (*D*) *H felis*. Cellular infiltrates (*arrows*), glandular hyperplasia (*triangles*), and follicular aggregates (*dotted lines*) can be observed in the mucosa of the animals (H&E stain; magnification ×20, scale bar 100 µm). Quantification of the (*E*) mucosal thickness and (*F*) numbers of mucosal follicles per gastric tissue section. (*G*) Detection of B and T lymphocytes within the gastric tissues of the mice using anti-mouse B220 (*left*) and anti-mouse CD3 (*right*) antibodies, respectively. B220$^+$ cellular infiltrates (*arrows*), mucosal follicles (*dotted lines*), and CD3$^+$ cells (*triangles*) can be observed. (magnification ×20, scale bar 100 µm). IgG-stained cells are shown as controls. Measurement of (*H*) the splenic weights (n = 10–42 mice per group) and *Helicobacter*-specific serum, (*I*) IgG, (*J*) IgA, (*K*) IgG1, and (*L*) IgG2c titers (n = 4–29 mice per group). In (*B*), (*C*), (*D*), (*E*), (*F*), and (*G*), at least 3 fields were analyzed per stomach. H&E images are representative of 20 to 30 mice per group. B220 and CD3 staining is representative of ≥6 mice. Data are presented as the mean ± SEM. Mann-Whitney test, **P* < .05, ***P* < .01, ****P* < .001, *****P* < .0001, and ns = not significant.

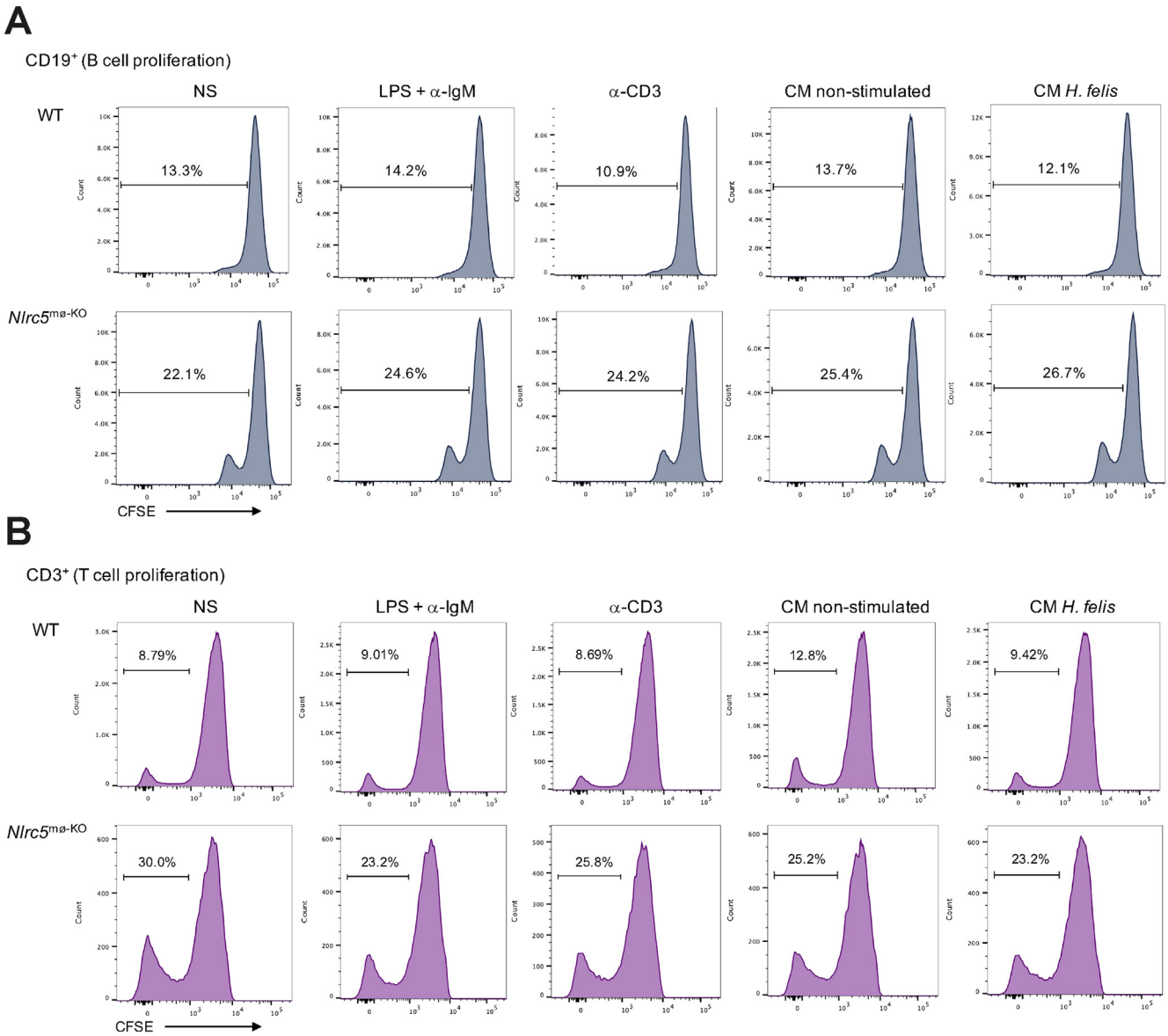

Figure 6. Increased proliferation in B- and T-splenocytes from *H felis*–infected *Nlrc5*$^{mø\text{-}KO}$ mice. Splenocytes from WT and *Nlrc5*$^{mø\text{-}KO}$ mice that had been infected with *H felis* for 3 months were assessed for (*A*) CD19^{+} and (*B*) CD3^{+} lymphocyte proliferation by flow cytometry. Carboxyfluorescein succinimidyl ester (CFSE)-labeled splenocytes were either not stimulated (NS) or treated with LPS + α-IgM (100 ng/mL), α-CD3 (100 ng/mL), or conditioned media (CM) from NS or *H felis*–stimulated (MOI 10) BMDMs. Splenocytes were analyzed 3 days poststimulation. Gated populations (*left side*) represent splenocytes that have undergone cell division, as observed by a reduction in CFSE staining. Gated populations on the *right side* represent the initial populations of CFSE-stained splenocytes on day 0. Data are representative of 3 independent experiments, of which ≥3 mice were used per group.

H felis–stimulated WT and *Nlrc5*$^{mø\text{-}KO}$ mice BMDMs were added to splenocytes of the corresponding genotype. As controls, splenocytes were either not stimulated or stimulated with either LPS + anti-IgM (α-IgM) or anti-CD3 (α-CD3), which act as a B-cell mitogen or activator of T cells, respectively. In response to stimulation, splenocyte-derived CD19^{+} and CD3^{+} populations from *Nlrc5*$^{mø\text{-}KO}$ mice proliferated at higher rates than WT cells across all treatment conditions (Figure 6 and Supplementary Figure 8). Similar observations were obtained for splenocytes from infected mice at 6 months p.i. (data not shown). These results suggest that *Nlrc5* deficiency in myeloid cells leads to enhanced B- and T-lymphocyte proliferation, and that NLRC5 may be responsible for regulating B- and T-cell proliferation in the spleen during *Helicobacter* infection.

Nlrc5$^{mø\text{-}KO}$ *BMDMs Secrete B- and T-cell Proliferative Factors in Response to* H felis

We showed that *NLRC5*$^{-/-}$ THP-1 macrophages secrete higher levels of BAFF in response to *H felis* stimulation compared with WT cells (Figure 4*A* and *B*). We therefore

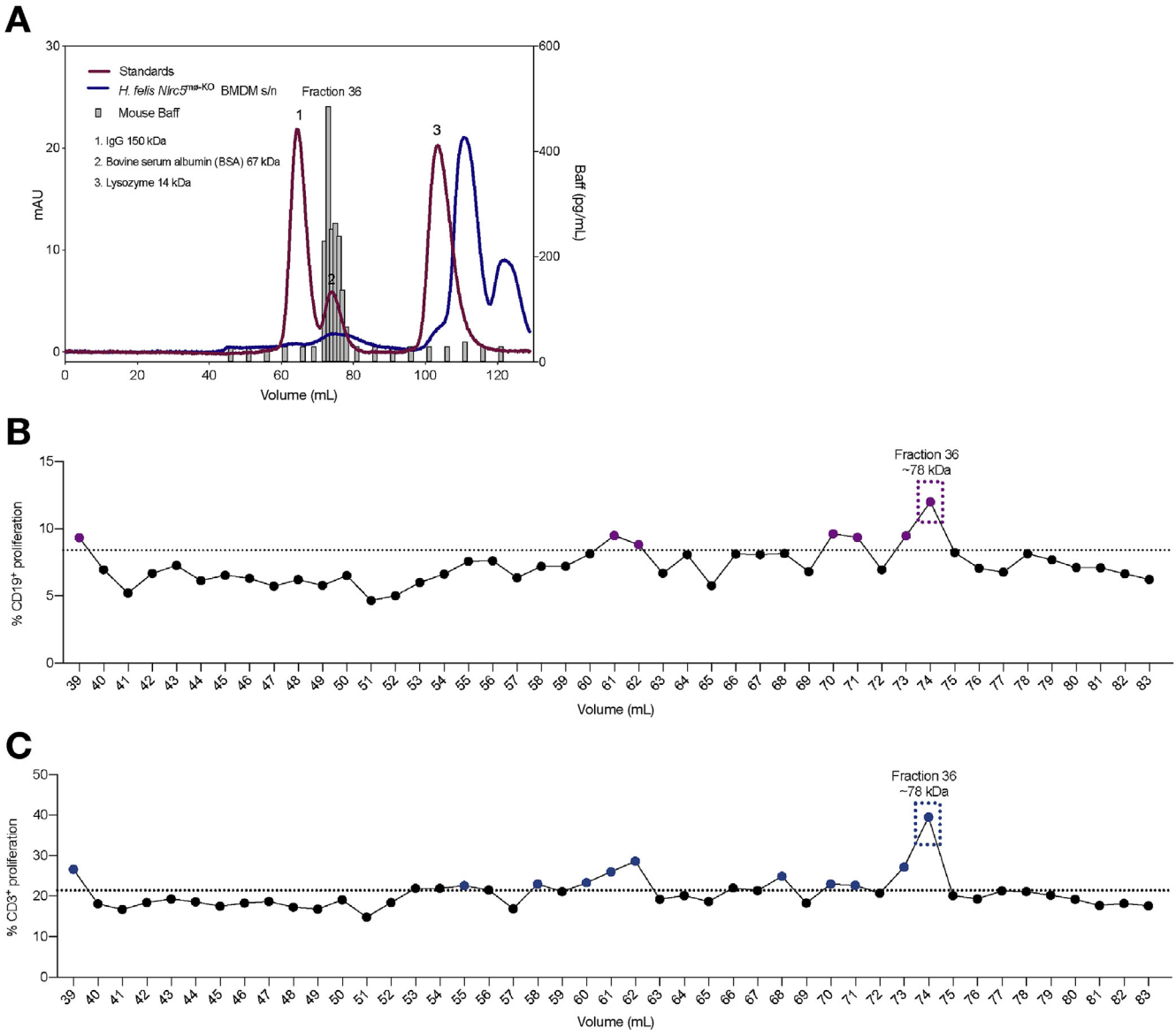

Figure 7. Macrophage-conditioned medium contains BAFF, which promotes B- and T-lymphocyte proliferation. *Nlrc5*$^{mø\text{-}KO}$ murine BMDMs were treated with *H felis* (MOI = 10) for 72 hours. The resulting BMDM-conditioned medium was concentrated and separated using size-exclusion chromatography. Fractions (1 mL) were collected. (*A*) Elution profiles (A_{280} nm) of the conditioned medium (*blue*) and protein standards (*red*). *Gray bars* show mouse BAFF levels (pg/mL, *left y-axis*) in fractions 8 to 83. CFSE-labeled *Nlrc5*$^{fl/fl}$ splenocytes were stimulated with fractions 1 to 45 for 72 hours. (*B*) $CD19^+$ and (*C*) $CD3^+$ proliferation of murine splenocytes. The *dotted line* along the *x-axis* represents baseline proliferation of nonstimulated splenocytes (8.39% for $CD19^+$ and 21.4% for $CD3^+$ cells). Data represent pooled splenocytes from 3 mice. *Dotted boxes* in (*A*) and (*B*) show the predicted eluted molecular weight of fraction 36. K_{av} values were calculated according to the equation: $K_{av} = V_e - V_o/V_t - V_0$, where V_e is the elution volume, V_0 is the void volume (40 mL), and V_t is the total bed volume (120 mL) of the column.

speculated that BAFF secretion by *H felis*–activated macrophages may drive the lymphocytic expansion observed in the *Nlrc5*$^{mø\text{-}KO}$ mice (Figure 5*C*–*E*, *G*). To investigate this question, *Nlrc5*$^{mø\text{-}KO}$ murine BMDMs were stimulated with *H felis* for 72 hours and the conditioned media subjected to size-exclusion chromatography. By testing pooled fractions for BAFF by ELISA, we detected peak BAFF activity in fractions 36 to 40 (data not shown). Individual fractions were then analyzed, revealing that BAFF was most abundant in fraction 36 (Figure 7*A*). To confirm that BAFF is the source of B- and T-cell proliferation in splenocytes and to investigate whether there may be additional factors present that induce cell proliferation, we tested fractions 1 to 45. Flow cytometry was used to determine $CD19^+$ B- and $CD3^+$ T-cell proliferation in carboxyfluorescein succinimidyl ester–labeled *Nlrc5*$^{fl/fl}$ splenocytes. Fraction 36 enhanced $CD19^+$ and $CD3^+$ proliferation compared with nonstimulated cells, indicating that BAFF in fraction 36 is one of the drivers of lymphocyte expansion (Figure 7*B* and *C*). This fraction is predicted to have an elution profile

consistent with a molecular mass of approximately 78 kDa. Interestingly, other fractions also induced moderate levels of B- and T-cell proliferation. This suggests that there may be other macrophage factors that drive B- and T-cell proliferation during *Helicobacter* infection. Taken together, we have shown that *Nlrc5*$^{mø\text{-}KO}$ murine macrophages secrete BAFF and other macrophage factors that induce B- and T-cell proliferation in response to *H felis*. Further studies to investigate whether these factors act synergistically to provide pro-proliferative signals to B or T cells alone, or whether cell proliferation is dependent on antigenic-activation through BCRs or involve ligand-ligand interactions via B- and T-cell interactions, will provide insight into the mechanisms of NLRC5-mediated B-cell lymphomagenesis during chronic *Helicobacter* infection.

Discussion

H pylori infection is a major causal factor in the development of gastric B-cell MALT lymphoma.[6] Many of the key pathogenetic mechanisms contributing to MALT lymphoma have been identified, yet the reasons why this neoplasm remains a relatively rare event among individuals with *H pylori* infection are unclear. Here, we identify intracellular NLRC5 to play a protective role against the development of B-cell follicular gastritis, a precursor to B-cell MALT lymphoma. Using the *H felis* mouse model, we show that animals lacking functional Nlrc5 in myeloid cells develop uncontrolled gastric B-cell lymphoid follicle formation. Our data suggest that gastric *Helicobacters* upregulate *NLRC5* expression in macrophages to dampen proinflammatory responses. *H felis* also induced the production of the B-cell proliferation and survival factor, BAFF. We propose that loss of NLRC5 function may predispose *H pylori*–infected individuals to gastric B-cell lymphomagenesis. This finding is consistent with recent whole-exome sequencing studies, linking modifications in the *NLRC5* locus with various cancers.[22,35,36]

NLRC5 expression was previously reported to occur in various mucosal tissues, such as the lung, small intestine, colon, and uterus.[18,19,29] Moreover, its expression was important in modulating CD8$^+$ T-cell responses against intestinal infections by *Listeria monocytogenes*[31] and rotavirus.[37] We found that *H pylori* infection was associated with significantly increased levels of *Nlrc5/NLRC5* expression in the stomach mucosa of infected hosts (Figure 1*A* and *B*). An important activator of *NLRC5* expression is the Type II IFN, IFN-γ (Figures 1 and 2),[18] which is produced locally during *H pylori* infection and is responsible for much of the immunopathology associated with the infection.[23] Consistent with this finding, *IFNG* expression was significantly increased in *H pylori*–positive gastric biopsies and correlated positively with both gastritis severity and *NLRC5* expression (Supplementary Figure 1). Nevertheless, we can exclude potential autocrine effects of IFN-γ on the responses of *NLRC5*$^{-/-}$ THP-1 macrophages to *Helicobacter* stimulation (Figure 3*J* and *K*).

Macrophages act as sentinel immune cell populations that regulate inflammation during *H pylori* infection.[9–11] As reported previously,[18,19,21] we found *Nlrc5*/*NLRC5* to be expressed strongly in myeloid cells, but now show that gastric epithelial cell lines also express this NLR (Figure 2 and Supplementary Figure 3). In contrast to our findings, one study described significant decreases in *NLRC5* expression in response to *H pylori* stimulation in THP-1 macrophages,[38] but expression was measured at 6 hours poststimulation, rather than the longer time-points used here. Once activated by *Helicobacter* infection, we observed that NLRC5 forms perinuclear aggregates in macrophages (Figure 2*C*), which is consistent with the reported interactions between NLRC5 and an inflammasome containing the NLR family pyrin domain-containing protein, NLRP3.[39] Nonetheless, in contrast to that study, which reported that NLRC5 positively regulates the inflammasome, in the *Helicobacter* infection model it would likely be a negative regulator (Figure 3*H*). Given that NLRC5 can shuttle between the cytosol and nucleus,[18] we propose that NLRC5 shuttling to the nucleus may regulate proinflammatory responses and MHC functions during *Helicobacter* infection. Consistent with the known role of NLRC5 as an MHC class I transactivator,[22,31,32,40] we observed significant upregulation of the MHC class I gene, *HLAB*, in *NLRC5*$^{-/-}$ THP-1 macrophages stimulated with *Helicobacter* bacteria when compared with WT cells (Figure 3*C*). In parallel, a compensatory and constitutive upregulation of the MHC class II gene, *HLADRB*, was observed in *NLRC5*$^{-/-}$ THP-1 cells (Figure 3*C*). This finding warrants further investigation, but may be attributed to the fact that NLRC5 and its analogous regulator, class II MHC transactivator, function via the same common DNA binding factors of the enhanceosome.[32]

Activation of the NF-κB pathway and induction of proinflammatory cytokines in host cells is important for *H pylori*–induced inflammation.[41,42] Here, we show that NLRC5 negatively regulates NF-κB–dependent chemokine/cytokine responses in both human and murine macrophages. Similarly, Benko et al[18] demonstrated that small-interfering RNA silencing of *Nlrc5* in RAW264.7 murine macrophages resulted in increased levels of IL-6, tumor necrosis factor, and IL-1β, coupled with a reduction in the anti-inflammatory cytokine, IL-10. In contrast, Kumar et al[20] found NLRC5 to be dispensable in cytokine responses against *Salmonella* and *Listeria* infection in mice. The observed differences for NLRC5 regulation of proinflammatory responses may be attributed to either cell-specific effects, the influence of multiple NLRC5 isoforms conferring distinct functions[21] and/or the gene-targeting strategies used to construct *Nlrc5*-deficient mice.[20,30,43] One of the key findings of the current work was the development of gastric mucosal hyperplasia and B-cell lymphoid follicles in *H felis*–infected *Nlrc5*$^{mø\text{-}KO}$ mice at just 3 months p.i. (Figure 5*C*–*G*). These results suggest that aberrant NLRC5 signaling in the myeloid lineage is associated with a dysregulation of the host immune response, leading to severe pathological changes in the host. Indeed, *Nlrc5*$^{mø\text{-}KO}$ mice with chronic *H felis* infection developed gastric lesions that were consistent with the B-cell–predominant lymphoid follicles that precede the development of human gastric MALT lymphoma.[5,6] In agreement with previous studies,[44] we also found that *H felis* induced

much more severe pathology than *H pylori* in the *Nlrc5*$^{mø\text{-}KO}$ model (Figure 5*C*–*G*). Strikingly, the B-cell lymphoid follicle formation in these mice occurred much more rapidly than in either *Helicobacter*-infected WT or thymectomized BALB/c animals, which typically develop such lesions at 22[7] and 12[45] months p.i., respectively. At 22 months p.i., 30% of *H felis*–infected BALB/c animals also developed lymphoepithelial lesions identical to those observed in human gastric MALT lymphoma.[7]

Nlrc5$^{mø\text{-}KO}$ mice with *Helicobacter* infection developed splenomegaly at 3 months p.i. (Figure 5*H*). These mice also had elevated levels of Th1 and Th2 type *Helicobacter*-specific serum antibody levels at $\geq$ 3 months p.i. (Figure 5*I*–*L*; MC, data not shown). These findings suggest that the innate immune molecule NLRC5 may shape adaptive immune responses and splenic functions during chronic *Helicobacter* infection. *NLRC5* is abundantly expressed in the spleen,[19] which is the site of B-cell development. *H pylori* is thought to drive B-cell clonal expansion through antigenic stimulation and prolonged inflammation in the gastric mucosa.[16] Neoplastic B and, more rarely, neoplastic T cells give rise to gastric MALT lymphoma, a low-grade neoplasia.[16] We speculate that *Helicobacter*-specific antigens drive the clonal expansion of B cells within the stomachs of the *Nlrc5*$^{mø\text{-}KO}$ mice. Indeed, splenocytes from *H felis*–infected *Nlrc5*$^{mø\text{-}KO}$ mice had increased B- and T-cell proliferation compared with WT mice, thus suggesting that both *Helicobacter*-specific B and T cells may act in a synergistic manner to drive monoclonal expansion of malignant cell populations within the gut mucosa. Hussell et al[16] found that B-cell proliferation was greatly reduced on removal of T cells in lymphocyte cultures from gastric MALT lymphoma patients on *Helicobacter* stimulation.

It has been shown that *H pylori* induces macrophage secretion of the B-cell pro-proliferative and cell-survival factors, BAFF and APRIL, associated with B-cell lymphomagenesis.[13,14,33] In our study, we provide evidence that NLRC5 in macrophages negatively regulates *BAFF* expression (Figure 4*A*) and protein production (Figure 4*A*) in response to *Helicobacter* stimulation, with *H felis* inducing higher levels of BAFF production than *H pylori*. Although APRIL and BAFF share some receptors, the 2 factors can have distinct biological roles and the functions of APRIL may be fulfilled by BAFF.[14,46] Based on these in vitro findings, we speculated that BAFF is the main driver of B-cell proliferation in *Nlrc5*$^{mø\text{-}KO}$ mice. By performing size-exclusion chromatography, we identified fractions in *H felis*–treated *Nlrc5*$^{mø\text{-}KO}$ BMDM-conditioned media that contained BAFF and mediated B- and T-splenocyte proliferation (Figures 6 and 7). These fractions eluted at an approximate molecular weight of 78 kDa (Figure 7), consistent with a BAFF-trimer, which is the most abundant form of systemic BAFF.[47] It is important to note, however, that BAFF may exist in multiple oligomeric forms (ie, -trimer, -60-mer) and can be either soluble or membrane-bound,[48] which may affect its biological activity.[47]

In conclusion, we show for the first time that myeloid-specific NLRC5 plays a homeostatic role in regulating the excessive inflammation that develops during chronic *Helicobacter* infection. We postulate that *H pylori* produces a factor that specifically targets NLRC5 in macrophages, thereby restraining NF-κB signaling and attenuating inflammation in the host. This NLRC5 regulation of proinflammatory signaling in macrophages shapes adaptive immune responses by controlling the secretion of B-cell promoting factors, such as BAFF, which in turn regulates B-cell lymphomagenesis in the gastric mucosa. Consistent with other reports,[22,35,36] we suggest that NLRC5 may act as a type of tumor suppressor in *H pylori*–induced B-cell gastric MALT lymphoma disease. Thus, this work identifies a potential new target for both novel intervention strategies and genetic screening of individuals who may be predisposed to MALT lymphomagenesis due to *H pylori*. Furthermore, these findings may be relevant to other infectious agents that promote MALT lymphoma, such as *Campylobacter jejuni*, *Borrelia burgdorferi,* or Epstein-Barr virus.[49]

Supplementary Material

Note: To access the supplementary material accompanying this article, visit the online version of *Gastroenterology* at www.gastrojournal.org, and at https://doi.org/10.1053/j.gastro.2020.03.009.

References

1. Maloy KJ, Powrie F. Intestinal homeostasis and its breakdown in inflammatory bowel disease. Nature 2011; 474:298–306.
2. Miller LS, O'Connell RM, Gutierrez MA, et al. MyD88 Mediates Neutrophil Recruitment Initiated by IL-1R but Not TLR2 Activation in Immunity against *Staphylococcus aureus*. Immunity 2006;24:79–91.
3. Pirofski LA, Casadevall A. Immune-mediated damage completes the parabola: *Cryptococcus neoformans* pathogenesis can reflect the outcome of a weak or strong immune response. MBio 2017;8.
4. Correa P, Haenszel W, Cuello C, et al. A model for gastric cancer epidemiology. Lancet 1975;306:58–60.
5. Zucca E, Bertoni F, Roggero E, et al. Molecular analysis of the progression from *Helicobacter pylori*–associated chronic gastritis to mucosa-associated lymphoid-tissue lymphoma of the stomach. N Engl J Med 1998;338:804–810.
6. Wotherspoon AC, Ortiz-Hidalgo C, Falzon MR, et al. *Helicobacter pylori*-associated gastritis and primary B-cell gastric lymphoma. Lancet 1991;338:1175–1176.
7. Enno A, O'Rourke JL, Howlett CR, et al. MALToma-like lesions in the murine gastric mucosa after long-term infection with *Helicobacter felis*. A mouse model of *Helicobacter pylori*-induced gastric lymphoma. Am J Clin Pathol 1995;147:217.
8. Ferrero RL, Avé P, Radcliff FJ, et al. Outbred mice with long-term *Helicobacter felis* infection develop both gastric lymphoid tissue and glandular hyperplastic lesions. J Pathol 2000;191:333–340.

9. Hardbower DM, Singh K, Asim M, et al. EGFR regulates macrophage activation and function in bacterial infection. J Clin Invest 2016;126:3296–3312.
10. Hardbower DM, Asim M, Luis PB, et al. Ornithine decarboxylase regulates M1 macrophage activation and mucosal inflammation via histone modifications. Proc Natl Acad Sci U S A 2017;114:E751–E760.
11. Kaparakis M, Walduck AK, Price JD, et al. Macrophages are mediators of gastritis in acute *Helicobacter pylori* infection in C57BL/6 mice. Infect Immun 2008;76:2235–2239.
12. Haeberle H, Kubin M, Bamford K, et al. Differential stimulation of interleukin-12 (IL-12) and IL-10 by live and killed *Helicobacter pylori* in vitro and association of IL-12 production with gamma interferon-producing T cells in the human gastric mucosa. Infect Immun 1997;65:4229–4235.
13. Munari F, Fassan M, Capitani N, et al. Cytokine BAFF released by *Helicobacter pylori*–infected macrophages triggers the Th17 response in human chronic gastritis. J Immunol 2014;193:5584–5594.
14. Munari F, Lonardi S, Cassatella MA, et al. Tumor-associated macrophages as major source of APRIL in gastric MALT lymphoma. Blood 2011;117:6612–6616.
15. Craig VJ, Arnold I, Gerke C, et al. Gastric MALT lymphoma B cells express polyreactive, somatically mutated immunoglobulins. Blood 2010;115:581.
16. Hussell T, Isaacson PG, Spencer J, et al. The response of cells from low-grade B-cell gastric lymphomas of mucosa-associated lymphoid tissue to *Helicobacter pylori*. Lancet 1993;342:571–574.
17. Fritz JH, Ferrero RL, Philpott DJ, et al. Nod-like proteins in immunity, inflammation and disease. Nat Immunol 2006;7:1250–1257.
18. Benko S, Magalhaes JG, Philpott DJ, et al. NLRC5 limits the activation of inflammatory pathways. J Immunol 2010;185:1681–1691.
19. Cui J, Zhu L, Xia X, et al. NLRC5 negatively regulates the NF-kappaB and type I interferon signaling pathways. Cell 2010;141:483–496.
20. Kumar H, Pandey S, Zou J, et al. NLRC5 deficiency does not influence cytokine induction by virus and bacteria infections. J Immunol 2011;186:994–1000.
21. Neerincx A, Lautz K, Menning M, et al. A role for the human nucleotide-binding domain, leucine-rich repeat-containing family member NLRC5 in antiviral responses. J Biol Chem 2010;285:26223–26232.
22. Yoshihama S, Roszik J, Downs I, et al. NLRC5/MHC class I transactivator is a target for immune evasion in cancer. Proc Natl Acad Sci U S A 2016;113:5999–6004.
23. Wroblewski LE, Peek RM, Wilson KT. *Helicobacter pylori* and gastric cancer: factors that modulate disease risk. Clin Microbiol Rev 2010;23:713–739.
24. Allison CC, Ferrand J, McLeod L, et al. Nucleotide oligomerization domain 1 enhances IFN-gamma signaling in gastric epithelial cells during *Helicobacter pylori* infection and exacerbates disease severity. J Immunol 2013;190:3706–3715.
25. Philpott DJ, Belaid D, Troubadour P, et al. Reduced activation of inflammatory responses in host cells by mouse-adapted *Helicobacter pylori* isolates. Cell Microbiol 2002;4:285–296.
26. Lee A, O'Rourke J, De Ungria MC, et al. A standardized mouse model of *Helicobacter pylori* infection: introducing the Sydney strain. Gastroenterology 1997;112:1386–1397.
27. Lee A, Hazell SL, O'Rourke J, et al. Isolation of a spiral-shaped bacterium from the cat stomach. Infect Immun 1988;56:2843–2850.
28. D'Costa K, Chonwerawong M, Tran LS, et al. Mouse models of *Helicobacter* infection and gastric pathologies. J Vis Exp 2018;140.
29. Kuenzel S, Till A, Winkler M, et al. The nucleotide-binding oligomerization domain-like receptor NLRC5 is involved in IFN-dependent antiviral immune responses. J Immunol 2010;184:1990–2000.
30. Tong Y, Cui J, Li Q, et al. Enhanced TLR-induced NF-[kappa]B signaling and type I interferon responses in NLRC5 deficient mice. Cell Res 2012;22:822–835.
31. Biswas A, Meissner TB, Kawai T, et al. Cutting edge: impaired MHC class I expression in mice deficient for Nlrc5/class I transactivator. J Immunol 2012;189:516–520.
32. Ludigs K, Seguín-Estévez Q, Lemeille S, et al. NLRC5 exclusively transactivates MHC Class I and related genes through a distinctive SXY module. PLoS Genet 2015;11. e1005088–e1005088.
33. Kuo SH, Yeh PY, Chen LT, et al. Overexpression of B cell-activating factor of TNF family (BAFF) is associated with *Helicobacter pylori*-independent growth of gastric diffuse large B-cell lymphoma with histologic evidence of MALT lymphoma. Blood 2008;112:2927–2934.
34. Chonwerawong M, Avé P, Huerre M, et al. Interferon-γ promotes gastric lymphoid follicle formation but not gastritis in *Helicobacter*-infected BALB/c mice. Gut Pathog 2016;8:61.
35. Li YY, Chung GTY, Lui VWY, et al. Exome and genome sequencing of nasopharynx cancer identifies NF-κB pathway activating mutations. Nat Commun 2017;8:14121.
36. Tiacci E, Ladewig E, Schiavoni G, et al. Pervasive mutations of JAK-STAT pathway genes in classical Hodgkin lymphoma. Blood 2018;131:2454–2465.
37. Sun T, Ferrero RL, Girardin SE, et al. NLRC5 deficiency has a moderate impact on immunodominant CD8(+) T-cell responses during rotavirus infection of adult mice. Immunol Cell Biol 2019;97:552–562.
38. Castano-Rodriguez N, Kaakoush NO, Goh KL, et al. The NOD-like receptor signalling pathway in *Helicobacter pylori* infection and related gastric cancer: a case-control study and gene expression analyses. PLoS One 2014;9:e98899.
39. Davis BK, Roberts RA, Huang MT, et al. Cutting edge: NLRC5-dependent activation of the inflammasome. J Immunol 2011;186:1333–1337.
40. Neerincx A, Jakobshagen K, Utermohlen O, et al. The N-terminal domain of NLRC5 confers transcriptional activity for MHC class I and II gene expression. J Immunol 2014;193:3090–3100.

41. Ferrero RL, Ave P, Ndiaye D, et al. NF-kappaB activation during acute *Helicobacter pylori* infection in mice. Infect Immun 2008;76:551–561.
42. van Den Brink GR, ten Kate FJ, Ponsioen CY, et al. Expression and activation of NF-kappa B in the antrum of the human stomach. J Immunol 2000; 164:3353–3359.
43. Robbins GR, Truax AD, Davis BK, et al. Regulation of Class I major histocompatibility complex (MHC) by nucleotide-binding domain, leucine-rich repeat-containing (NLR) proteins. J Biol Chem 2012;287:24294–24303.
44. Sakagami T, Dixon M, O'Rourke J, et al. Atrophic gastric changes in both *Helicobacter felis* and *Helicobacter pylori* infected mice are host dependent and separate from antral gastritis. Gut 1996;39:639–648.
45. Chrisment D, Dubus P, Chambonnier L, et al. Neonatal thymectomy favors *Helicobacter pylori*–promoted gastric mucosa-associated lymphoid tissue lymphoma lesions in BALB/c mice. Am J Pathol 2014;184:2174–2184.
46. Varfolomeev E, Kischkel F, Martin F, et al. APRIL-deficient mice have normal immune system development. Mol Cell Biol 2004;24:997–1006.
47. Bossen C, Cachero TG, Tardivel A, et al. TACI, unlike BAFF-R, is solely activated by oligomeric BAFF and APRIL to support survival of activated B cells and plasmablasts. Blood 2008;111:1004–1012.
48. Cachero TG, Schwartz IM, Qian F, et al. Formation of virus-like clusters is an intrinsic property of the tumor necrosis factor family member BAFF (B cell activating factor). Biochemistry 2006;45:2006–2013.
49. Suarez F, Lortholary O, Hermine O, et al. Infection-associated lymphomas derived from marginal zone B cells: a model of antigen-driven lymphoproliferation. Blood 2006;107:3034–3044.

Received August 27, 2019. Accepted March 3, 2020.

Correspondence
Address correspondence to: Richard L. Ferrero, PhD, Centre for Innate Immunity and Infectious Diseases, Hudson Institute of Medical Research, 27-31 Wright Street, Clayton, Melbourne, Victoria (3168), Australia. e-mail: Richard.Ferrero@Hudson.org.au; fax: 61-3-95947114.

Acknowledgments
We thank Jeanette Rientjes (Monash Genome Modification Platform, Monash University) for designing the gene-targeting strategy and generation of the *Nlrc5*$^{fl/fl}$ mice. Construction of these mice was funded in part by the Public Health Agency of Canada. We also acknowledge the Monash Histology Platform (Monash University, Monash Health Translation Precinct) for assisting with tissue processing for histology work; Julia Como, Amanda DePaoli, and Georgie Wray-McCann for their help with animal work. Christian Ferrero is thanked for his graphical assistance.

CRediT Authorship Contributions
Michelle Chonwerawong, Bsc (Hons) (Conceptualization: Supporting; Data curation: Lead; Formal analysis: Supporting; Investigation: Lead; Methodology: Lead; Writing –original draft: Lead; Writing – review & editing: Supporting). Jonathan Ferrand, PhD (Conceptualization: Supporting; Data curation: Lead; Formal analysis: Supporting; Investigation: Lead; Methodology: Lead; Project administration: Supporting; Resources: Lead). Hassan Mohammad Chaudhry, Bsc (Hons) (Investigation: Supporting)

Chloe Higgins, MBBS (Hons) (Data curation: Supporting; Formal analysis: Supporting; Investigation: Supporting; Validation: Lead). Le Son Tran, PhD (Conceptualization: Supporting; Data curation: Supporting; Formal analysis: Supporting; Investigation: Supporting; Supervision: Lead). San Sui Lim, PhD (Resources: Supporting; Supervision: Supporting). Marjorie Walker, MBBS (Investigation: Supporting; Resources: Supporting).

Prithi S. Bhathal, MBBS, PhD (Investigation: Supporting; Resources: Supporting). Anouk Dev, MBBS (Investigation: Supporting; Resources: Lead; recruitment of subjects, sample collection: Lead). Gregory Moore, MBBS (Resources: Supporting; recruitment of subjects, sample collection: Supporting). William Sievert, MBBS (Resources: Supporting; recruitment of subjects, sample collection: Supporting). Brendan J. Jenkins, PhD (Resources: Supporting; recruitment of subjects, sample collection: Supporting). Mario D'Elios, PhD (Resources: Supporting; recruitment of subjects, sample collection: Supporting). Dana J. Philpott, PhD (Resources: Supporting; expertise: Supporting). Thomas A Kufer, PhD (Resources: Supporting; Writing – review & editing: Supporting; expertise: Supporting). Richard Louis Ferrero, PhD (Conceptualization: Lead; Formal analysis: Supporting; Funding acquisition: Lead; Investigation: Supporting; Project administration: Lead; Supervision: Lead; Writing – original draft: Supporting; Writing – review & editing: Lead).

Conflict of interest
The authors disclose no conflicts.

Funding
Construction of the *Nlrc5*$^{fl/fl}$ mice was funded in part by the Public Health Agency of Canada. The work in Richard L. Ferrero's laboratory was funded by the National Health and Medical Research Council (Project grants APP1011303 and APP1107930; Senior Research Fellowship, APP1079904) and the US Department of Defense (Award No. W81XWH-17–1–0606). Michelle Chonwerawong is the recipient of a Monash International Postgraduate Research Scholarship and a Monash Graduate Scholarship from the Faculty of Medicine, Nursing and Health Sciences, Monash University. Research at the Hudson Institute of Medical Research is supported by the Victorian Government's Operational Infrastructure Support Program.

Supplementary Materials and Methods

Immunofluorescence

PMA-treated WT and *NLRC5*$^{-/-}$ THP-1 cells were fixed with 4% (wt/vol) paraformaldehyde for 15 minutes at room temperature. Cells were washed in phosphate-buffered saline (PBS) and blocked in 3% bovine serum albumin (wt/vol) and 0.1% (wt/vol) saponin in PBS, then incubated overnight at 4°C with rat anti-human NLRC5 antibody clone 3H8 (1:1000; Merck Millipore, Boston, MA). Samples were washed thrice with blocking buffer and incubated with anti-rat Alexa Fluor 488-conjugated secondary antibody (1:400) for 2 hours at room temperature. As controls, staining with primary antibody was omitted and cells were only stained with secondary antibody alone. Cells were washed, then cell nuclei were stained with Hoechst 33342 (1:1000; Thermo Fisher Scientific, Waltham, MA) for 5 minutes before mounting with DPX mounting media (Sigma-Aldrich, St Louis, MO). Imaging was performed on an Olympus FV1200 confocal microscope using a ×20 objective, and acquired using the FluoView FV10a software (Olympus, Melbourne, Australia). Figures were generated using FIJI software (version 1.0; University of Wisconsin-Madison, WI). All images are representative of 3 fields of view from a minimum of 2 replicates per treatment group.

Western Blot

Cell lysates were prepared using 50 μL of lysis buffer per well (500 μL of 2 × RIPA buffer [100 mM TRIS-HCl pH8, 300 mM NaCl, 2% Triton-X, 1% sodium deoxycholate, 0.2% SDS, 2 mM EDTA], 25 μL of 40 × protease inhibitor cocktail [Roche], 1 μL of 1000 × phosphate inhibitor cocktail [Roche], 474 μL of H_2O). Total protein lysates (50 μg), determined using the Qubit fluorometer (Thermo Fisher Scientific), were resuspended in Laemmli buffer (Thermo Fisher Scientific) and loaded onto NuPAGE 4% to 12% gels run at 120 V in 1 × MES buffer (Thermo Fisher Scientific). Gels were transferred onto membranes using the iBlot transfer system. (Thermo Fisher). Membranes were blocked in Odyssey blocking buffer (Li-cor, Lincoln, NE) for 2 hours, then incubated at 4°C overnight in rat anti-human NLRC5 antibody (Clone3H8, 1:1000; Merck Millipore) or rabbit anti-phospho-signal transducer and activator of transcription 1 (STAT1; Tyr701, Clone 58D6, 1:3000; Cell Signaling Technology, Danvers, MA). Membranes were then washed in PBS Tween-20 (PBST) (0.05% [vol/vol] Tween 20 in PBS) and incubated in either goat anti-rat IgG DyLight 800 (Rockland, Limerick, PA) or anti-rabbit IgG DyLight 680 (Rockland), respectively, at 1:3000 dilution for 2 hours at room temperature. Washing was repeated, then membranes were analyzed using the Odyssey Infrared Imaging System. Mouse monoclonal anti-β-Actin antibody (Clone AC-15; Sigma-Aldrich) or rat anti-tubulin antibody (Clone YL1/2; Abcam, Cambridge, UK) were used as loading controls.

Immunohistochemistry

Paraffin-embedded gastric tissue sections were dewaxed in xylene and ethanol. Antigen retrieval was performed by immersing slides in 10 mM sodium citrate buffer (pH 6.0) then heating slides in a microwave for 2 to 3 minutes, until boiling, followed by low power for 10 minutes. Slides were left to cool completely, then endogenous peroxidase blocked by treatment with 3% H_2O_2 in methanol. Sections were blocked for a minimum of 1 hour with 10% (vol/vol) goat serum (Vectastain Elite ABC-HRP Kit; Vector Laboratories, Burlingame, CA) in PBS or CAS block (Invitrogen, Carlsbad, CA), for CD3 or B220 staining, respectively. Purified rat anti-mouse anti-CD45R B220 antibody (BD Biosciences) was diluted 1:2000 in CAS block. Rabbit anti-mouse CD3 (SP7) (Abcam) was diluted 1:1000 in 10% goat serum in PBS. As controls, tissue sections were stained with anti-mouse IgG (1:200; Vectastain). Sections were washed with PBST, incubated in the appropriate secondary antibody (1:500; BioLegend, San Diego, CA) and washed in PBST before applying Vectastain (VECTASTAIN Elite ABC-HRP Kit; Vector Laboratories). Sections were washed, incubated in DAB chromogen (Dako, Glostrup, Denmark), then washed in distilled water and counterstained with Harris' hematoxylin (Amber Scientific). Images were analyzed using an Olympus DP73 digital camera and CellSens Dimension software.

In Vitro B- and T-Lymphocyte Proliferation of Murine Splenocytes

Spleens from mice were collected in RPMI supplemented with 10% fetal calf serum, 1% P/S, and 1% L-glutamine. Single cell suspensions were prepared using 70-μm cell strainers and recovered in RPMI media, before labeling with 5 μM carboxyfluorescein succinimidyl ester (CFSE) (Invitrogen) for 10 minutes, then washed in cRPMI. Cells were seeded in 12-well plates in duplicate or triplicate at 5 × 10^5 cells/mL. Labeled splenocytes were incubated at 37°C in 5% CO_2 for a minimum of 1 hour, then left untreated or treated with either 100 ng/mL *Escherichia coli* O111: B4 lipopolysaccharide (LPS) (UltraPure; InvivoGen, San Diego, CA) and 100 ng/mL purified mouse anti-IgM antibody (Clone RMM-1; BioLegend), 100 ng/mL mouse anti-CD3ε antibody (Southern Biotech, Birmingham, AL) or conditioned media from primary murine BMDMs. Splenocytes were incubated at 37°C in 5% CO_2 for 72 hours, then harvested and washed with ice-cold Dulbecco's phosphate-buffered saline (DPBS) (Gibco, Waltham, MA) by centrifugation at 200*g* for 5 minutes, followed by 2 more washes with FACS buffer (5% fetal calf serum in DPBS). Splenocytes were stained with propidium iodide (PI, 1:1000) (Invitrogen), TruStain fcX anti-mouse CD16/CD32 antibody (1:100, BioLegend), Pacific Blue anti-mouse CD3 antibody (Clone 17A2; 1:100; BioLegend), and APC anti-mouse CD19 antibody (Clone 1D3/CD19; 1:100; BioLegend). Cell proliferation was assessed by flow cytometry (Canto II Analyzer; BD Biosciences). Compensation set up and data acquisition were performed on a FACSCanto system (BD Biosciences) using nonstained and single-stained cells. Flow cytometry analyses were performed using Kaluza Flow Cytometry Analysis software (Beckman and Coulter, Inc., Brea, CA).

Identification of Lymphocyte-Inducing Macrophage Factors

Size-exclusion chromatography was performed on *H felis*–treated BMDM culture supernatants from *Nlrc5*$^{mø\text{-}KO}$ mice (72 hours poststimulation). The supernatants were concentrated using Vivaspin 20 centrifugal concentrators (10 kDa; Sartorius, Gottingen, Germany) and washed in PBS (pH 7.4) supplemented with protease inhibitors (cOmplete, Mini, EDTA-free Protease Inhibitor Cocktail; Roche, Basel, Switzerland). Samples were loaded onto a HiLoad Superdex 200-pg 16/600 column (GE Healthcare Life Sciences, Little Chalfont, UK) connected to an ÄKTAprime plus chromatography system (GE Healthcare Life Sciences). Fractions (1 mL) were eluted in PBS starting from an elution volume of 39 mL to 130 mL for the last fraction collected (ie, fraction 1 = elution volume 30 mL). Collected fractions were stored at 4°C for downstream analyses. A standard run was performed using the following proteins of known molecular weights: IgG monoclonal antibody (150 kDa, made "in-house"); bovine serum albumin (67 kDa); and lysozyme (14 kDa), both from Sigma-Aldrich.

Spleens were collected, processed, and labeled with CFSE, as described previously. Splenocytes were seeded at a density of 2×10^4 cells/well in U-bottom 96-well plates and stimulated for 72 hours at 37°C in 5% CO_2 with 25-μL aliquots of chromatography fractions from *H felis*–treated *Nlrc5*$^{mø\text{-}KO}$ BMDM supernatants. Before labeling of cells for flow cytometry, splenocytes were washed by centrifuging the 96-well culture plates at 200*g* for 5 minutes at 4°C. Cell pellets were resuspended in fresh, ice-cold FACS buffer, then washed twice in FACS buffer. Splenocytes were stained with TruStain fcX anti-mouse CD16/CD32 (1:100; BioLegend), Pacific Blue anti-mouse CD3 (Clone 17A2; 1:100; BioLegend), and APC anti-mouse CD19 (Clone 1D3/CD19; 1:100; BioLegend) antibodies, respectively, for 30 minutes on ice. Stained cells were washed twice with FACS buffer and resuspended in 300 μL FACS buffer. Before sample acquisition, PI (1:1000; Invitrogen) was added to labeled cells. Compensation set up and data acquisition was performed on a FACSCanto system (BD Biosciences) using nonstained and single-stained cells. Data were analyzed using FlowJo Software (BD Biosciences).

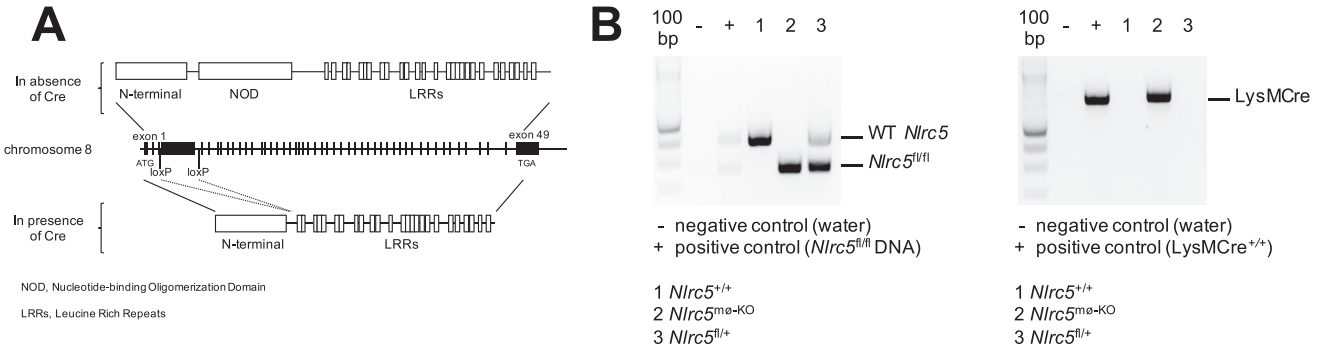

Supplementary Figure 1. Conditional deletion of *Nlrc5* in the myeloid cell compartment. (*A*) Schematic representation showing the construction of *Nlrc5*$^{mø\text{-}KO}$ mice using Cre-Lox recombination. *Nlrc5* is located on chromosome 8 of the mouse genome and contains a central NOD/NACHT domain that is encoded by exon 4 and is required for NLR signaling. *Nlrc5* "floxed" (*Nlrc5*$^{fl/fl}$) mice were generated by the insertion of *loxP* sites adjacent to the 5′ and 3′ ends of exon 4. *Nlrc5*$^{fl/fl}$ mice were crossed with Cre-expressing animals, resulting in *Nlrc5*$^{mø\text{-}KO}$ mice that lack a fully functional Nlrc5 in the myeloid cell lineage. (*B*) Genotyping results demonstrating "floxing" of *Nlrc5* (*left*, lane 2) and expression of LysM-Cre in an *Nlrc5*$^{mø\text{-}KO}$ mouse (*right*, lane 2).

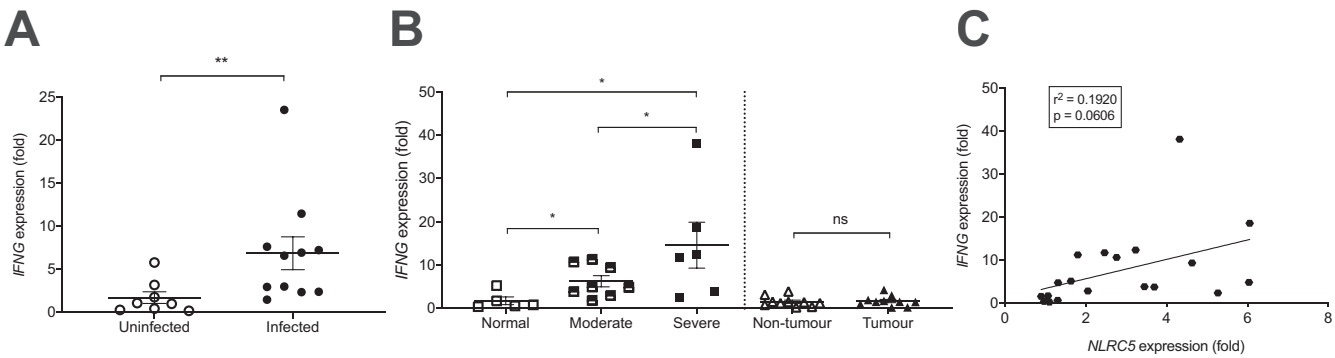

Supplementary Figure 2. *IFNG* expression is upregulated in human gastric biopsies in response to *H pylori* infection and gastritis severity. (*A*) *IFNG* expression in human gastric biopsies from individuals with or without *H pylori* infection. (*B*) *IFNG* expression in biopsies scored by histopathology as being either "normal" or displaying gastritis of varying severity, as well as those showing adenocarcinoma development (paired tumor and nontumor samples). (*C*) Spearman correlation test for *IFNG* and *NLRC5* expression in *H pylori*–infected human gastric biopsies. Gene expression levels were determined by qRT-pCR and normalized to the uninfected group. Data are presented as the mean ± SEM. Values for individual human gastric tissue samples are presented (n = 5–11 individuals/group). Mann-Whitney test: $^{*}P < .05$, $^{**}P < .01$.

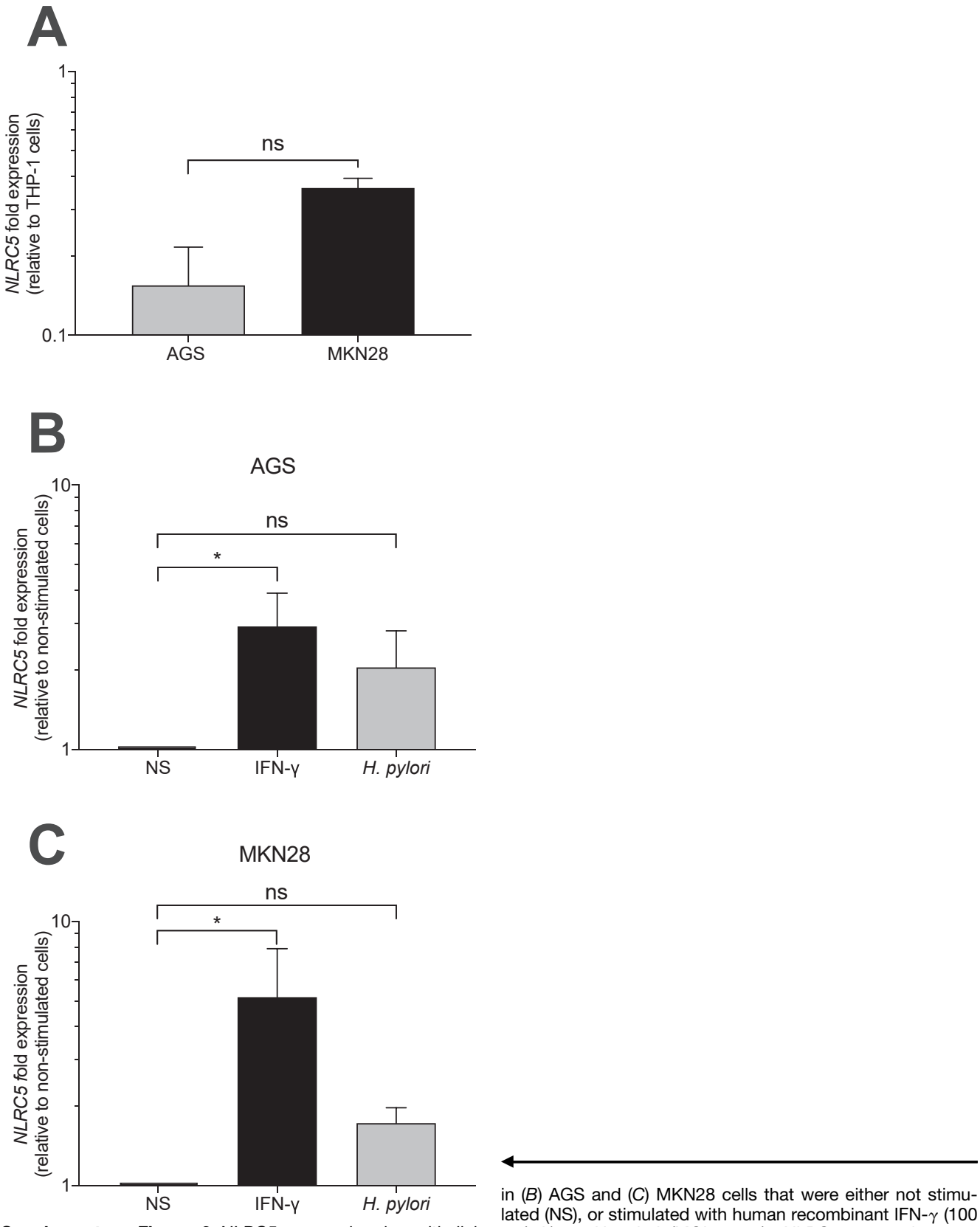

Supplementary Figure 3. *NLRC5* expression in epithelial cells and macrophages. (*A*) Relative *NLRC5* expression in unstimulated AGS and MKN28 human gastric epithelial cell lines. *NLRC5* expression was normalized to that in human monocyte-derived THP-1 macrophages. *NLRC5* expression in (*B*) AGS and (*C*) MKN28 cells that were either not stimulated (NS), or stimulated with human recombinant IFN-γ (100 ng/mL) or *H pylori* (MOI $=$ 10). *NLRC5* expression was normalized to nonstimulated cells. Data are presented as mean $\pm$ SEM from 3 to 6 independent experiments. Mann-Whitney or Kruskal-Wallis tests, as appropriate: *$P < .05$ and ns $=$ not significant.

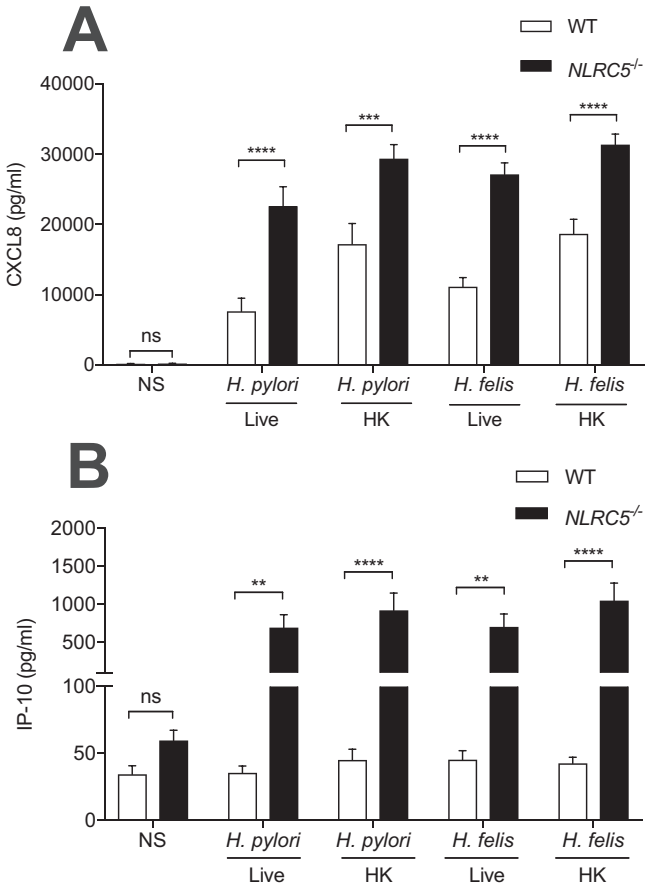

Supplementary Figure 4. Nonviable *Helicobacter* bacteria induce increased chemokine production in *NLRC5*$^{-/-}$ macrophages. Monocyte-derived WT and *NLRC5*$^{-/-}$ THP-1 macrophages were either not stimulated (NS) or stimulated with human recombinant IFN-γ (100 ng/mL), LPS (100 ng/mL), *H pylori* SS1, or *H felis* (MOI = 10). Bacteria were either viable (live) or heat-killed (HK). Levels of (*A*) CXCL8 and (*B*) CXCL10 in cell culture supernatants were determined at 24 hours poststimulation. Data are presented as the mean ± SEM from 3 independent experiments. Two-way analysis of variance: ** $P < .01$, *** $P < .001$, **** $P < .0001$, and ns = not significant.

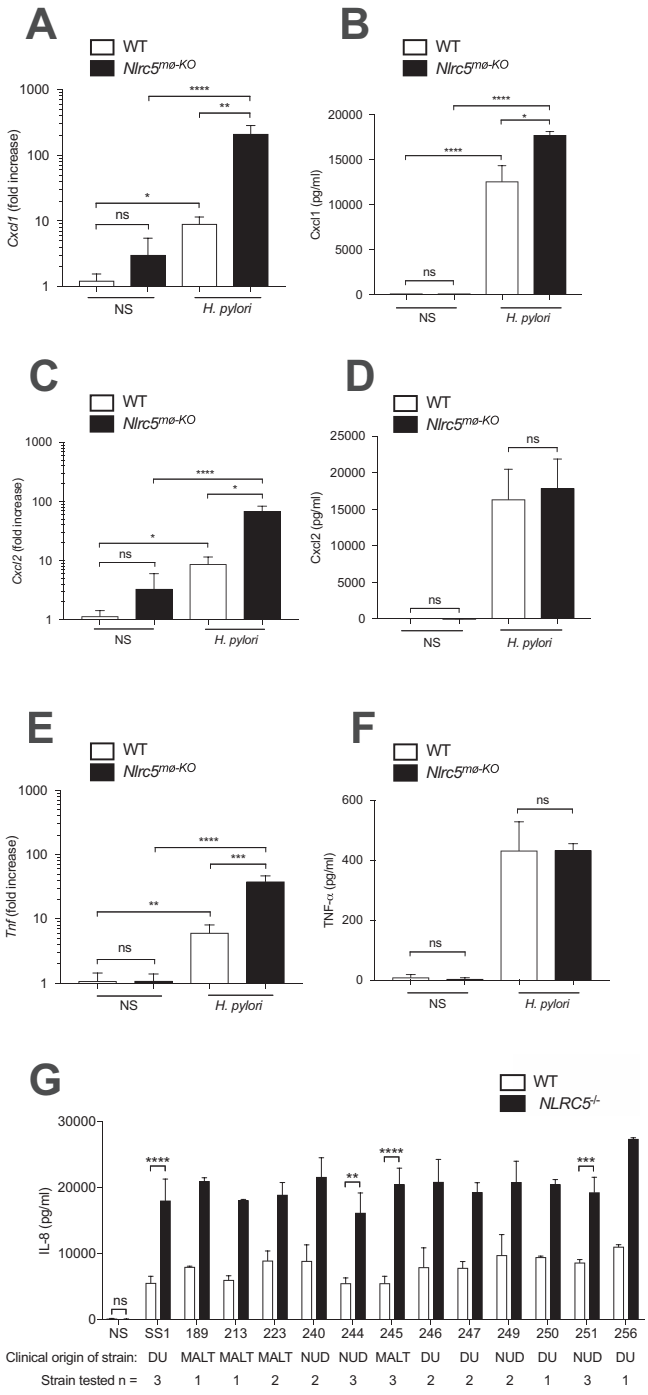

Supplementary Figure 5. Enhanced proinflammatory cytokine responses in *Nlrc5*/*NLRC5*-defective macrophages to *H pylori* stimulation. BMDMs from WT and *Nlrc5*$^{\text{mø-KO}}$ mice were either not stimulated (NS) or stimulated with *H pylori* and then assayed for the following responses: (*A*) *Cxcl1*, (*B*) Cxcl1/KC, (*C*) *Cxcl2*, (*D*) Cxcl2/MIP-2, (*E*) *Tnf* and (*F*) TNF-α. (*G*) CXCL8 responses in monocyte-derived WT and *NLRC5*$^{-/-}$ THP-1 macrophages that were either not treated (NS) or stimulated with *H pylori* strains associated with different clinical outcomes, as follows: mucosa-associated lymphoid tissue (MALT; 189, 213, 223, 245), nonulcer dyspepsia (NUD; 240, 244, 249, 251), and duodenal ulcer (DU; SS1, 246, 247, 250, 256) (Philpott, 2002 #87)[25]. Data are presented as the mean ± SEM from 3 independent experiments. For (*G*): n = 1 for strains 189, 213, 250. 256; n = 2 for strains 223, 240, 246, 247, 249; n = 3 for *H pylori* SS1, *H felis*, 244, 245, 251 (statistical analyses were only performed for n =3 data). Two-way analysis of variance: $^{**}P < .01$, $^{***}P < .001$, $^{****}P < .0001$.

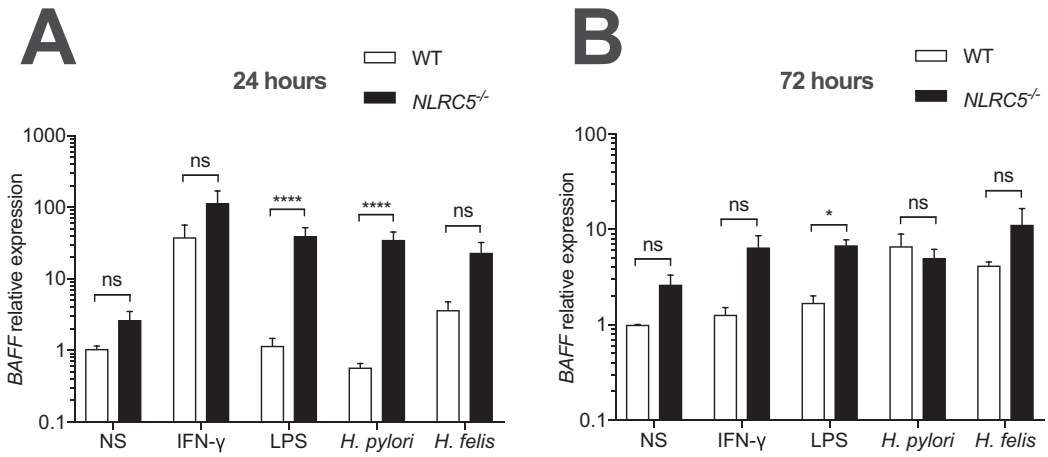

Supplementary Figure 6. *NLRC5*$^{-/-}$ THP-1 cells exhibit increased *BAFF* expression in response to stimulation. *BAFF* expression was measured in monocyte-derived WT and *NLRC5*$^{-/-}$ THP-1 macrophages at (*A*) 24 and (*B*) 72 hours post-stimulation with human recombinant IFN-γ (100 ng/mL), LPS (100 ng/mL), *H pylori* SS1, or *H felis* (MOI = 10). Expression levels were normalized to those of nonstimulated cells (NS). Data are presented as the mean ± SEM from 3 independent experiments. Two-way analysis of variance: **P* < .05, *****P* < .0001, and ns = not significant.

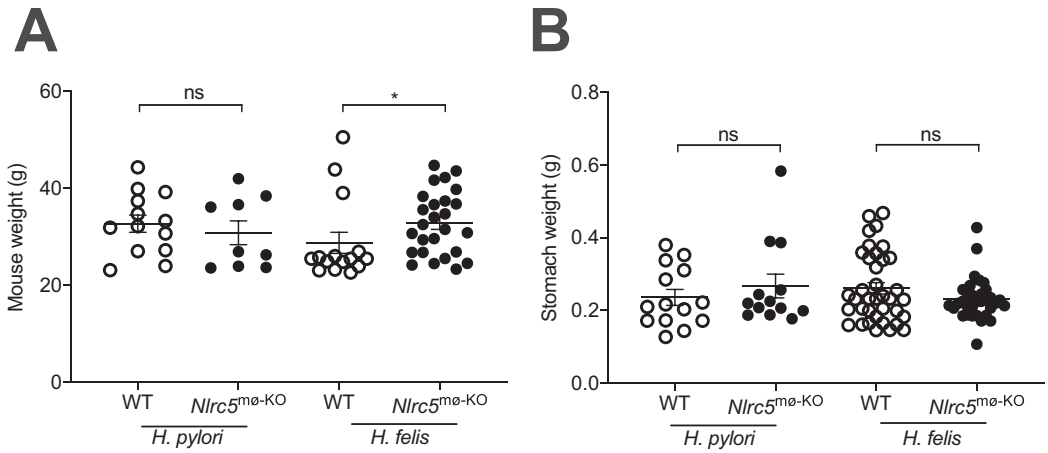

Supplementary Figure 7. Body and stomach weights of WT and *Nlrc5*$^{mø\text{-}KO}$ mice infected with *H pylor*i SS1 or *H felis*. (*A*) Mouse and (*B*) stomach weights were recorded at 3 months postinfection. Stomach contents were emptied and the stomachs washed in sterile PBS before measurement. Each value represents measurements from 1 mouse (n ≥ 9 mice/group). Data are presented as the mean ± SEM. Mann-Whitney test: **P* < .05, ns = non-significant.

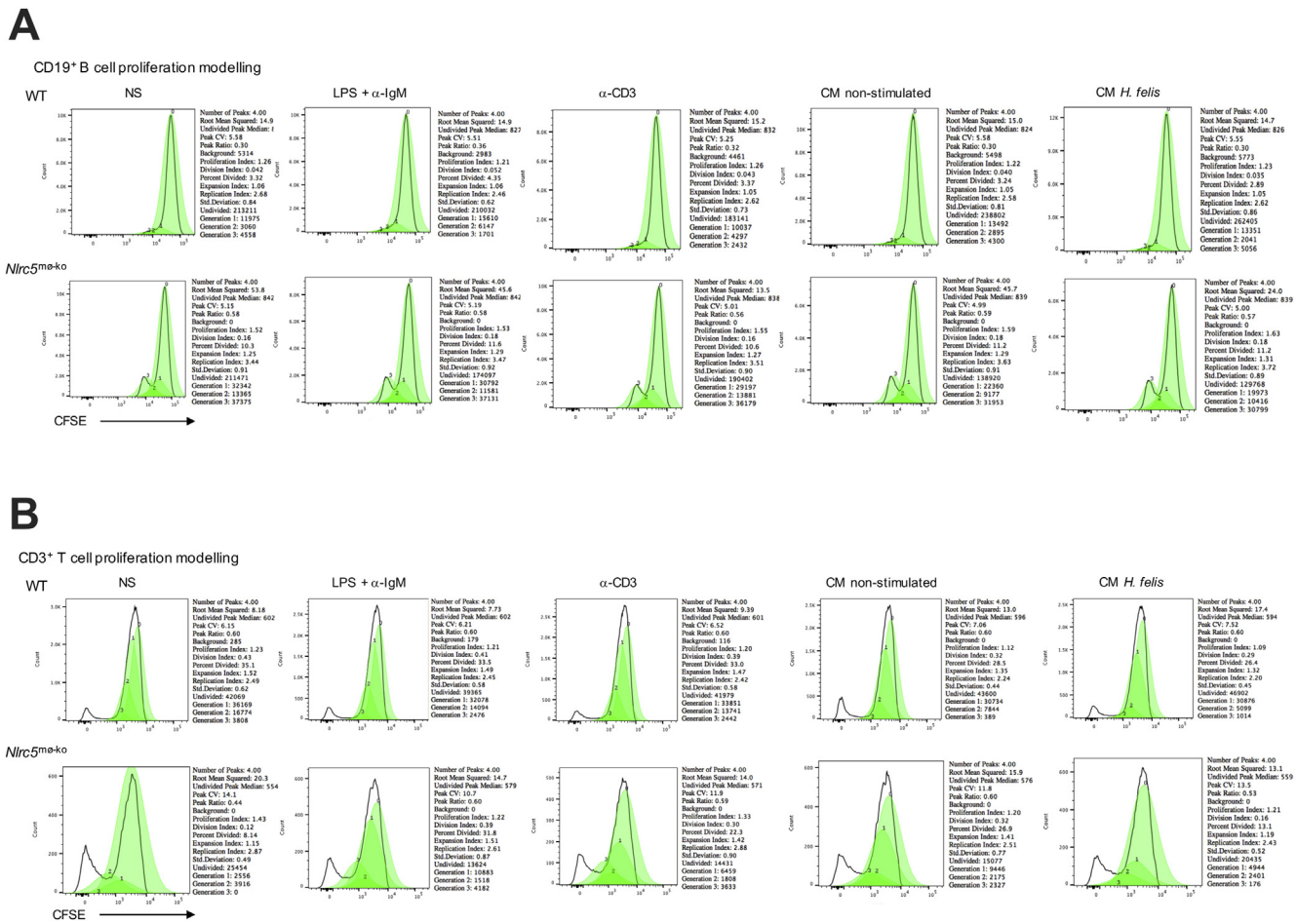

Supplementary Figure 8. Increased proliferation in B- and T-splenocytes from *H felis*–infected *Nlrc5*$^{mø\text{-}KO}$ mice. Splenocytes from WT and *Nlrc5*$^{mø\text{-}KO}$ mice that had been infected with *H felis* for 3 months were assessed for (*A*) CD19^{+} and (*B*) CD3^{+} lymphocyte proliferation by flow cytometry. CFSE-labeled splenocytes were either not stimulated (NS) or treated with LPS + α-IgM (100 ng/mL), α-CD3 (100 ng/mL), or conditioned media (CM) from NS or *H felis*–stimulated (MOI = 10) BMDMs. Splenocytes were analyzed 3 days poststimulation. Gated populations (*left*) represent splenocytes that have undergone cell division, as observed by a reduction in CFSE staining. Gated populations on the *right side* represent the initial populations of CFSE-stained splenocytes on day 0. Presented are data for cell replication, division, and proliferation peaks, as well as the number of peaks in each sample. Data are representative of 3 independent experiments, of which $\geq$3 mice were used per group.